Universidad del País Vasco
Euskal Herriko Unibertsitatea
BILBOKO INGENIARITZA ESKOLA
ESCUELA DE INGENIERÍA DE BILBAO

MÁSTER UNIVERSITARIO EN

INGENIERÍA INDUSTRIAL

TRABAJO FIN DE MÁSTER

DESIGN OF GREEN HYDROGEN PRODUCTION FROM OFFSHORE WIND ENERGY

Estudiante *Ainz Galindez, Oihane*
Director/Directora *Herrero Villalibre, Saioa*
Departamento
Curso académico *2021/2022*

Bilbao, 5 de septiembre de 2022

CRANFIELD UNIVERSITY

OIHANE AINZ GALINDEZ

DESIGN OF GREEN HYDROGEN PRODUCTION FROM OFFSHORE WIND ENERGY

SCHOOL OF WATER, ENERGY AND ENVIRONMENT
Renewable Energy MSc

MSc
Academic Year: 2021 – 2022

Supervisor: Professor Phil Longhurst
Associate Supervisor: Dr Peter Clough
September 2022

CRANFIELD UNIVERSITY

SCHOOL OF WATER, ENERGY AND ENVIRONMENT
Renewable Energy MSc

MSc

Academic Year 2021 - 2022

OIHANE AINZ GALINDEZ

Design of green hydrogen production from offshore wind energy

Supervisor: Professor Phil Longhurst
Associate Supervisor: Dr Peter Clough
September 2022

This thesis is submitted in partial fulfilment of the requirements for the degree of Renewable Energy MSc

ABSTRACT

Establishing hydrogen production infrastructure from renewable energy is a high priority for the energy transition. This project analyses options for deployment using offshore wind generation to power electrolysis for green hydrogen production. A case example of northern Spain is used to examine the optimisation and sensitivity of trade-offs between generator and electrolysis locations, as well as electricity and hydrogen transport. Both, onshore and offshore electrolyser locations are analysed.

Using this case example enables demonstration of the logical sequence of infrastructure development priorities; an assessment of the critical locations for renewable energy; and most importantly an improved understanding of the sensitivity of different assumptions used to complete the whole system analysis. To this end, a sensitivity analysis is carried out using @RISK software to define the reliability of the results obtained, as well as the key factors that dominate the decision-making in the system design.

The study concludes by presenting a decision-making tool to determine the optimum location of both the wind farm and the electrolyser, as well as the transport method for the case site to achieve the established requirements and an assessment of resilience for the outline system design.

Keywords:

Offshore wind energy, floating offshore wind, levelized cost of energy (LCOE), feasibility study, site selection, green hydrogen, PEM electrolysis, alkaline electrolysis, energy transport, sensitivity analysis.

ACKNOWLEDGEMENTS

I would like to express my gratitude to my project supervisors, Professor Phil Longhurst and Dr Peter Clough for their support, guidance, and advice during these challenging months. I would also like to thank Cranfield University and the Faculty of Engineering Bilbao (UPV/EHU) for giving me the opportunity to participate in this Double Degree programme. I would also like to highlight the help and support received from Petronor, both through the Enrique Sendagorta Scholarship, without which this experience would not have been possible, and through their participation in this project. Lastly, I would like to thank my family and friends for listening to me and helping me, both in good and bad times, as well as for all the support they have given me, without which I would not be here today.

TABLE OF CONTENTS

LIST OF FIGURES

LIST OF TABLES

LIST OF EQUATIONS

LIST OF ABBREVIATIONS

AE	Alkaline Electrolyser
BH_2C	Basque Hydrogen Corridor
CAPEX	Capital Expenditures
CGH_2	Compressed hydrogen
CO_{2eq}	Carbon Dioxide Equivalent
D&C	Development and Consenting
DES	Direct Electrolysis of Seawater
EU	European Union
GHG	Greenhouse Gas
HVAC	High Voltage Alternating Current
HVDC	High Voltage Direct Current
LCOE	Levelized Cost of Energy
LH_2	Liquid hydrogen
LNG	Liquefied Natural Gas
LOHC	Liquid Organic Hydrogen Carriers
NPV	Net Present Value
O&M	Operation and Maintenance
OPEX	Operating Expenses
PEM	Proton Exchange Membrane
R&D	Research and Development
RO	Reverse Osmosis
SOE	Solid Oxide Electrolyser
TLP	Tension Leg Platform

1 INTRODUCTION

1.1 Background of study

Renewable hydrogen is a key energy carrier for the decarbonisation of the economy, which will make it possible to achieve climate neutrality by 2050 and develop a high-value-added economy in both the European Union (EU) and Spain.

Hydrogen is expected to penetrate sectors that are difficult to decarbonise and electrify, such as high-temperature processes, maritime transport, and hydrogen-intensive industry, among others. In the short term, industries that use hydrogen as feedstock, mainly oil refineries and chemical industries, have great potential to boost green hydrogen [1].

Within this context, Petronor, the largest refinery in Spain [2], has developed the Petronor Sustainability Plan 2021-2025 [3] which describes the company's strategy to meet its objective of supplying energy in a safe, efficient, accessible, and sustainable manner in line with the United Nations Sustainable Development Goals.

To this end, Petronor expects to achieve an 80-90% reduction in net emissions through improved energy efficiency, the use of carbon capture, and the production of renewable hydrogen, among others [3]. Concerning hydrogen production, three targets have been set [4]:

- **2021:** installation of a 2.5 MW electrolyser, the first step towards the development of renewable hydrogen in the Basque Country (Spain).
- **2024:** installation of a 10 MW electrolyser to supply Petronor's synthetic fuels manufacturing plant.
- **2025:** installation of a 100 MW electrolyser to tackle Petronor's decarbonisation process and supply the needs of the Basque Hydrogen Corridor (BH_2C).

The BH_2C [5] is a cluster made up of 78 organisations, including Petronor, whose aim is to boost the decarbonisation of strategic sectors such as energy, mobility, industry, and services. The creation of clusters will play a crucial role in the development of renewable hydrogen, since, by taking advantage of economies of scale, the technology can be developed to optimise its production, transport, and consumption [1].

At the same time, to enable renewable hydrogen production growth, it is essential to increase renewable electricity generation through technologies such as solar or wind [1]. This project analyses the feasibility of coupling offshore wind power generation and hydrogen production in the North-Atlantic region of Spain.

1.2 Aims and objectives

This project aims to understand the dominant factors that influence the decision-making on designing a hydrogen production system from renewable energy, as well as the interconnections between them.

The following objectives have been set to achieve this aim:

1. Design a 50 MW electrolyser by defining its characteristics and energy demand; and study the possible locations, including offshore installation.
2. Design a renewable electricity generation system according to site characteristics: evaluation of the available wind resource on the Spanish Cantabrian and Atlantic Coasts.
3. Optimisation of trade-offs between energy generation and electrolysis location, as well as electricity and hydrogen transport.
4. Evaluation of the uncertainty and resilience of the project, as well as the parameters that dominate the system.

1.3 Thesis structure

The decarbonisation of the economy implies fossil fuel use reduction and energy carriers development, which directly affects the Oil and Gas companies' operations that must adapt to the energy transition. This project contributes to this transition by analysing options for the deployment of green H_2 production from offshore wind energy.

A literature review has been carried out in Chapter 2, beginning with an understanding of the EU and Spanish legislative framework to decarbonise the economy by 2050. Besides, offshore wind technology, electrolysers types, and hydrogen transport are analysed.

Chapter 3, corresponding to the Methodology, details the procedure carried out in this project. Starting with the definition of the electrolyser's energy demand, passing through the sizing of the wind offshore farm, as well as the study of the viability of offshore H_2 production, and ending with an assessment of the system resilience.

Chapter 4, Results and Discussion, shows the outcomes of the study, such as the evaluation of the different sites for power generation and H_2 production, as well as a general discussion. Finally, Chapter 5 gives concluding remarks and recommendations for future work.

2 LITERATURE REVIEW

2.1 Regulatory framework

This section analyses the targets and measures established at European Union (EU) and Spanish levels to achieve climate neutrality by 2050. Additionally, the role of renewable hydrogen and offshore wind in meeting these targets is studied.

2.1.1 Framework for achieving Net-Zero emissions by 2050

Through the European Green Deal [6] and following the Paris Agreement [7] the EU aims to be climate neutral by 2050, meeting the objective of keeping average global temperature growth below 2 ºC and striving to limit the increase to 1.5 ºC, compared to pre-industrial levels (1990). To this end, the Member States have developed an action plan with a minimum time horizon of 30 years [8].

In this context, the Spanish Government has composed two roadmaps: the Integrated National Energy and Climate Plan 2021-2030 [9] for the short-medium term, and the Long-Term Decarbonisation Strategy 2050, which sets targets for 2050 [8].

Among the objectives of the Integrated National Energy and Climate Plan 2021-2030 [9] are to achieve 74% renewable electricity generation and 42% renewable energy production out of final energy consumption, achieving a 23% reduction of greenhouse gas (GHG) emissions compared to 1990. Besides, energy efficiency is expected to improve by 39.5%. These measures will also lead to a reduction in energy and fossil fuel dependency.

The Long-Term Decarbonisation Strategy 2050 [8] provides a roadmap for achieving climate neutrality by 2050, setting targets to be completed by 2030, 2040, and 2050. The main milestones to be achieved by 2050 are a 90% reduction of GHG emissions (compared to 1990), electrification of 50% of the economy, 97% contribution of renewable energies to final energy, and 100% renewable electricity production. All this leads to a significant reduction in external energy dependence, from 74% of energy imports in 2018 to 61% in 2030 and 13% in 2050. To achieve these targets, it is required to increase renewable power capacity (around 250 GW will be installed) and to develop hydrogen and renewable fuels.

2.1.2 Green hydrogen development

The European Green Deal [6] and the European Union Hydrogen Strategy [10] outline guidelines for the development of renewable hydrogen in the coming years in the EU, setting out three-time horizons:

- **First phase 2020-2024:** installation of at least 6 GW of electrolysers and production of up to 1 million tonnes of green H_2 with the objective of decarbonising current hydrogen consumption, mainly in refineries and steel and chemical production plants.
- **Second phase 2025-2030:** installation of at least 40 GW of electrolysers and production of up to 10 million tonnes of H_2, allowing hydrogen to penetrate the economy and become an indispensable mainstay.
- **Third phase 2030-2050:** the technology is expected to reach maturity penetrating sectors difficult to decarbonise.

The increase in electrolyser power implies the growth of renewable electricity generation, as it is expected that by 2050, around 25% of the electricity generated will be used for H_2 production [8].

In Spain, the Hydrogen Roadmap [1] describes the country's opportunities and objectives for developing this energy carrier. In addition to reducing pollutant emissions, hydrogen contributes to improving the degree of manageability of renewable energies. By 2030, an installed electrolyser capacity of 4 GW is foreseen, reaching a minimum renewable H_2 contribution of 25% of total industry H_2 consumption in Spain. This will reduce GHG emissions by 4.6 Mt in the 2020-2030 period. To achieve these targets, investments of up to 8.9 B€ are planned and the creation of hydrogen clusters is encouraged.

Furthermore, it is essential to increase renewable energy generation, for which Spain has advantageous climatic conditions, both solar and wind [1]. Moreover, the Roadmap Offshore Wind and Marine Energy in Spain report [11] points to Spain as one of the European countries with the greatest potential for exporting renewable energy, including hydrogen.

2.1.3 Offshore wind development

The EU Offshore Renewable Energy Strategy [12] sets out the roadmap for offshore wind and ocean energy (tidal and wave). Europe currently has 12 GW of offshore wind and 13 MW of marine energy, and this is expected to increase to 300 GW and 40 GW respectively by 2050 [12] which represents 15% and 11% of the projected global capacity [13].

The Roadmap Offshore Wind and Marine Energy in Spain [11] defines the Spanish strategy for the development of these technologies. Although marine energy is still in a pre-commercial stage, the development of offshore wind and floating platforms is making its installation on Spain's deep coast viable.

Spain is the second European country and the fifth in the world with the largest installed wind capacity and is among the three European countries with the highest R&D investment in the sector. Therefore, the knowledge acquired in the development of onshore wind could be applied to boost offshore wind deployment [11].

Although to date there is no offshore wind power installed in Spain, due to the narrow Spanish continental shelf [11], new floating concepts have made it possible to extend the geographical limits of exploitable marine areas beyond the depths of around 50 m [14] allowed by fixed foundations, reaching depths of up to 1,000 m [14], multiplying the areas of potential development off the Spanish coast.

Table 2-1: Targets for offshore wind installation in Spain [11]

	Objectives Spain 2030	Reference 2030
Offshore wind	1-3 GW (floating)	5-30 GW global floating 7 GW Europe floating 60 GW Europe fixed + floating

The Spanish coast is divided into 5 marine demarcations (Figure 2-1) in which renewable technologies could be implemented maximising the use of resources and protecting the marine environment. This project focuses on the analysis of the North-Atlantic subdivision.

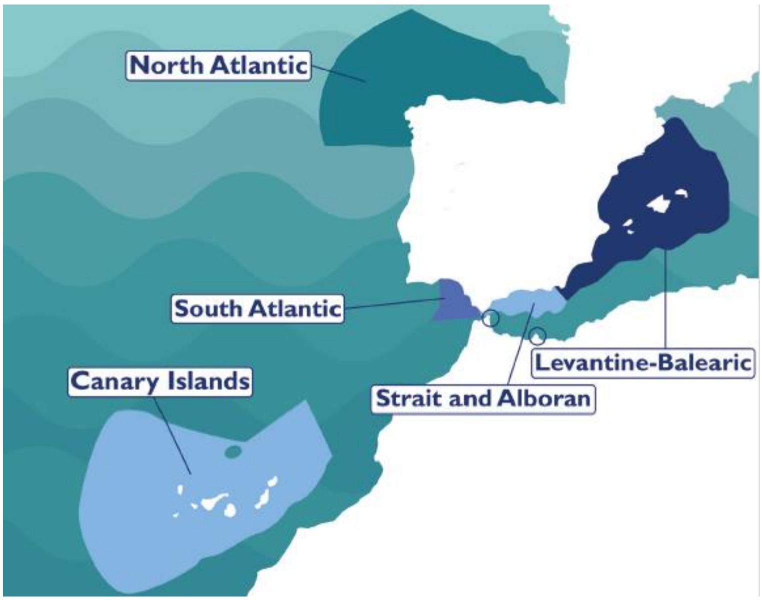

Figure 2-1: Spanish marine subdivisions [11]

2.2 State of the art

2.2.1 Offshore wind technology

Offshore wind turbines operate on the same principle as onshore wind turbines, although have been modified to withstand marine climatic conditions, especially corrosion. Besides, the support structure and tower have temperature and humidity regulation systems to reduce the internal corrosion risk [11].

The quality of offshore wind is superior to onshore in terms of average speed, energy density, and regularity due to the lack of obstacles, allowing the turbines to generate energy for longer periods. Therefore, to obtain the same power as on land, towers of lower height and blade dimensions are sufficient [11].

The wind map in Figure 2-2 shows the average wind speed in Spain and Portugal. As can be seen, on average, the wind speed is higher offshore than onshore and large areas with the same resource are available. To deploy an offshore wind farm, an average speed of 7 m/s is needed (at 100 m height), instead of the 6 m/s that would be sufficient to realise the project on land [15], [16].

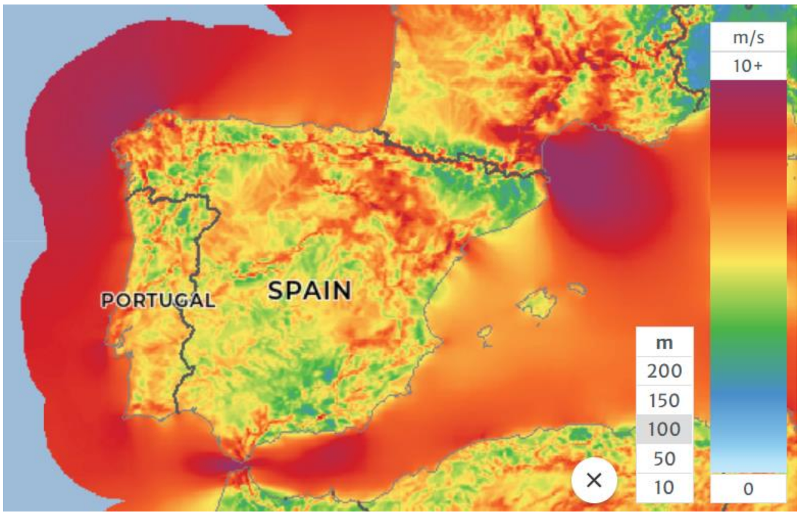

Figure 2-2: Wind map of Spain and Portugal [17]

Due to reduced spatial constraints, both turbine size and spacing can be increased, reducing wake losses. Therefore, new 10-12 MW turbines could reach capacity factors of over 50% [18], while in 2018 the global average capacity factor for offshore wind was 33%, 25% in the case of onshore wind, and compared to other renewables, solar photovoltaics only reached 14% [11]. In addition to increased power generation, a high capacity factor offers greater uniformity in production, contributing to the security of supply and better and more consistent utilisation of infrastructure.

The main difference between onshore and offshore wind turbines lies in the support structure, which can be classified into two main groups: fixed and floating. Their use depends mainly on the depth of the site. Fixed structures (monopile, jacket, or tripod [19]) are valid for locations up to 50 m deep [14], while floating structures can be installed on sites up to 1,000 m depth [20]. Figure 2-3 shows a map of bathymetry in Europe. As can be seen, only floating systems can be installed on the Spanish coast, due to its great depth.

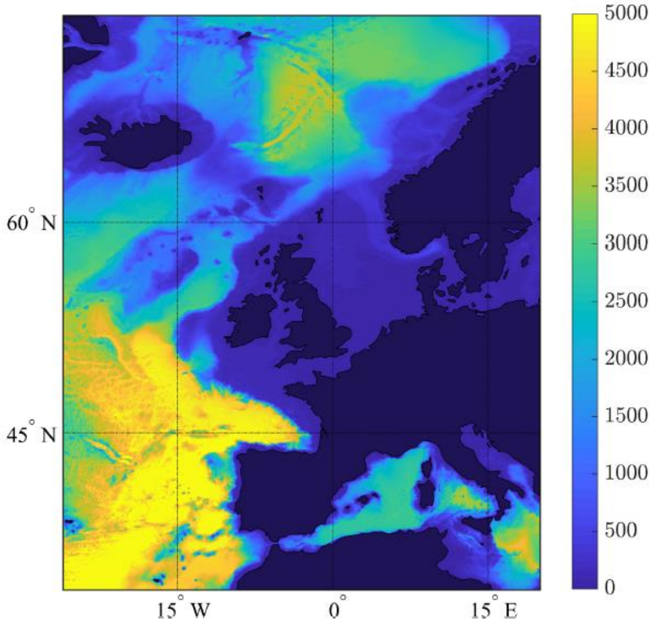

Figure 2-3: Bathymetry map of Europe [m] [21]

Floating structures can be further classified into three main groups (Figure 2-4) according to the stability principle used [22]: semisubmersible, tension leg platforms (TLP), and spar platforms.

Figure 2-4: Classification of floating offshore structures [23]

Semi-submersible platforms rely on the buoyancy principle and use catenary mooring lines to support the turbine. The main advantages of this system are depth independency [22] and ease of installation, as they can be installed on land for subsequent wet transport [23].

TLPs use mooring lines with suction pile anchors to stabilise the system. These structures are suitable for depths between 50 m and 120 m [14] and have low wave sensitivity and footprint [22]. Installation is challenging and the anchors used are expensive and complex [22], [23].

Spar platforms are ballasted with embedded catenary drag anchors, being suitable for deep water (> 120 m [14]). However, assembly, transport, and installation are difficult [23].

In addition to wind characteristics and bathymetry, other considerations such as navigation corridors, fishing banks, fishing grounds, seismic fault lines, environmental protected areas, rocky areas, distance to ports, and distance to shipyards must be considered to determine suitable areas for wind farms [20], [24], [25].

Several articles study both, the location constraints and the economic costs associated with the installation of a floating offshore wind farm in the North-Atlantic subdivision of Spain. However, the results obtained are very disparate, which creates the need to carry out a location study considering the specific data of the project to be developed.

In a study published in 2019, Castro-Santos et al. [26] analysed suitable areas for the installation of an offshore wind farm on the Galician coast (Atlantic region). The study was carried out to meet the restrictions mentioned above (Figure 2-5) and considered only semi-submersible platforms. Maximum NPV of around 350 M€ and minimum payback periods of 7 years were obtained for an installed power of 107 MW. Nonetheless, a second study [20] for the same wind farm, but considering different floating platforms, led to NPVs of 71.4 M€ for semisubmersible, 63.76 M€ for spar, and 38.73 M€ for TLP structures. In neither of the three solutions, not even 20.4% of the first study results were matched even though no location restrictions were considered in this case.

Furthermore, a third study [21] investigated floating offshore wind farm costs on the European Atlantic Coast. In this analysis, a wind farm composed of a hundred 10 MW turbines supported on semisubmersible platforms was studied without taking into account environmental restrictions, fishing areas, or navigation corridors, among others. This study resulted in LCOE values ranging between 100 and 135 €/MWh, while in the Gulf of Biscay values of 160 €/MWh were achieved. If these values are compared with the second study on the Galician coast the difference ranges from 42.1% to 84% (in the Gulf of Biscay) highlighting the need for more specific and actual research on the location for this project.

Figure 2-5: Suitable areas for offshore wind farm installation [25]

2.2.2 Renewable hydrogen production

The production of renewable hydrogen from offshore wind energy is an alternative that contributes to the coupling of sectors, increasing their efficiency and grid flexibility [11]. Hydrogen is not a primary energy source but an energy carrier that requires an energy input to be obtained and can store and release energy [1].

Hydrogen can be classified into different types depending on the materials used and the CO_2 emissions generated in its production. Green or renewable hydrogen is mainly obtained from water and electricity through the electrolysis process, which consists of the dissociation of the water molecule into oxygen and hydrogen through an electricity supply [1], [26]. Approximately 10 kg of high-purity water is required for each kilogram of hydrogen produced [27].

The main types of electrolysers are as follows:

- **Alkaline Electrolyser (AE):**

The electrolyte is an alkaline solution, usually NaOH or KOH [26], [28]. It is the most common and mature technology offering the lowest capital cost [28]. However, disadvantages include leakage problems [28], lower achievable current density [26], performance deterioration under part-load performance, and lower hydrogen production [28].

- **Proton Exchange Membrane Electrolyser (PEM):**

A solid polymer is used as the electrolyte, solving the leakage problem of alkaline-type electrolysers [28]. This type is also more compact [26], offers high current density and hydrogen can be produced at high pressures, omitting the use of a compressor. Besides, it can operate even under partial load conditions. However, it requires high voltage and distinct materials to operate under acidic conditions [28].

- **Solid Oxide Electrolyser (SOE):**

It has a solid electrolyte made from ceramic materials, reducing manufacturing costs and offering a more compact design [26]. It also eliminates the leakage problem. This type of electrolyser operates at high temperatures, which reduces the electricity requirements [28].

The electrolysers mentioned above require extremely pure water for their operation [27]. Therefore, if seawater is to be used as feedstock, it must first be desalinated by reverse osmosis (RO), multi-stage flash distillation, electrodialysis, or multiple effect desalination in addition to an ion-exchange electrodeionisation process [27].

On the other hand, direct electrolysis of seawater (DES) has the advantage that the electrolyte is the seawater itself. However, the current density is low, expensive materials are used (platinum and ruthenium) and the technology is under development [26].

Table 2-2 shows a comparison of the above-mentioned electrolyser types:

Table 2-2: Comparison of electrolyser types [26], [27]

	DES	AE	PEM	SOE
Cell voltage [V]	4	1.7-1.8	1.7-1.8	1.3
Current density [mA/cm^2]	10	100-300	1,000-2,000	1,000
System efficiency [%]	-	65-71	63-68	74-81
Lifetime [h]	10,000	100,000	100,000	10,000
Investment cost [€/kW]	6,000	400-850	600-1,300	2,000
O&M costs per annum [%]	4-5	2-6	3-5	-
Pressure [bar]	-	< 30	30-80	-
Temperature [ºC]	20	60-90	20-80	700-1,000

Moreover, the resistance to impurities in the feed water, the specific energy for hydrogen production at sea, and the swiftness of response to sudden power changes should also be analysed [28]. This last point is of special interest when the electrolyser is supplied with electricity produced by renewable technologies, as the power output is not constant but source dependent.

Thus, the coupling of wind turbine technology and electrolysis systems raises several challenges in terms of power supply. Since the wind speed is not constant, there are fluctuations in the power produced by the turbine. When the power is lower than that of the electrolysers, they would operate at partial load, which could deteriorate their performance (this effect affects mainly alkaline electrolysers) [28].

On the other hand, it can also happen that the power produced by the turbines is higher than the nominal power of the electrolyser, since, the nominal power of the wind farm must be higher than that of the electrolyser, for it to operate as many hours as possible. The system must be designed to maximise the power used and minimise the power wasted [28].

2.2.3 Hydrogen storage and transport

Hydrogen can be transported in a gaseous or liquid state, or by liquid carriers:

- **Compressed hydrogen (CGH_2):** H_2 is a very low-density gas, which makes it expensive to store on a large scale and transport over long distances [1], [29]. However, this property facilitates its storage under pressure (compressed hydrogen). It could also be injected into the gas grid by blending, although this would imply a loss of the renewable character of hydrogen and the separation of the gases would pose technical difficulties.
- **Liquid hydrogen (LH_2):** Similar to liquefied natural gas (LNG), hydrogen can be transported and stored by liquefying it at -253 ºC, improving energy density and storage efficiency [30].
- **Hydrogen carriers such as ammonia or organic liquids (LOHC):** Hydrogen can be transformed into easily transportable liquid substances (methanol, octane, or ammonia and organic liquids) using existing supply lines. When hydrogen is to be used, the liquid is dehydrogenated [29].

Hydrogen is typically transported and stored as CGH_2 or LH_2 [29]. Disadvantages of CGH_2 include high tank costs and low energy density, whereas LH_2 has a higher energy density, but the liquefaction costs are very high [29].

Small-scale hydrogen storage, for short-term use, is mainly done by high-pressure tanks (200-1,000 bar), although the main limitation is their reduced volume [1], [30]. Sometimes metals are used, which in the presence of hydrogen, form metal hydrides that store hydrogen. The suitability of the compound to absorb/release hydrogen depends on parameters such as charge/discharge pressure and temperature or process speed [1].

When H_2 volumes are too large to be stored in reservoirs, the use of natural geological storage such as salt caverns, aquifers, or depleted natural gas or oil reservoirs is considered, suitable for the long-term [1], [31].

When deciding on the most appropriate transport method to be used in a project, both the hydrogen status and the transport method must be considered. Figure 2-6 shows the transport costs based on the distance and the volume of H_2 transported:

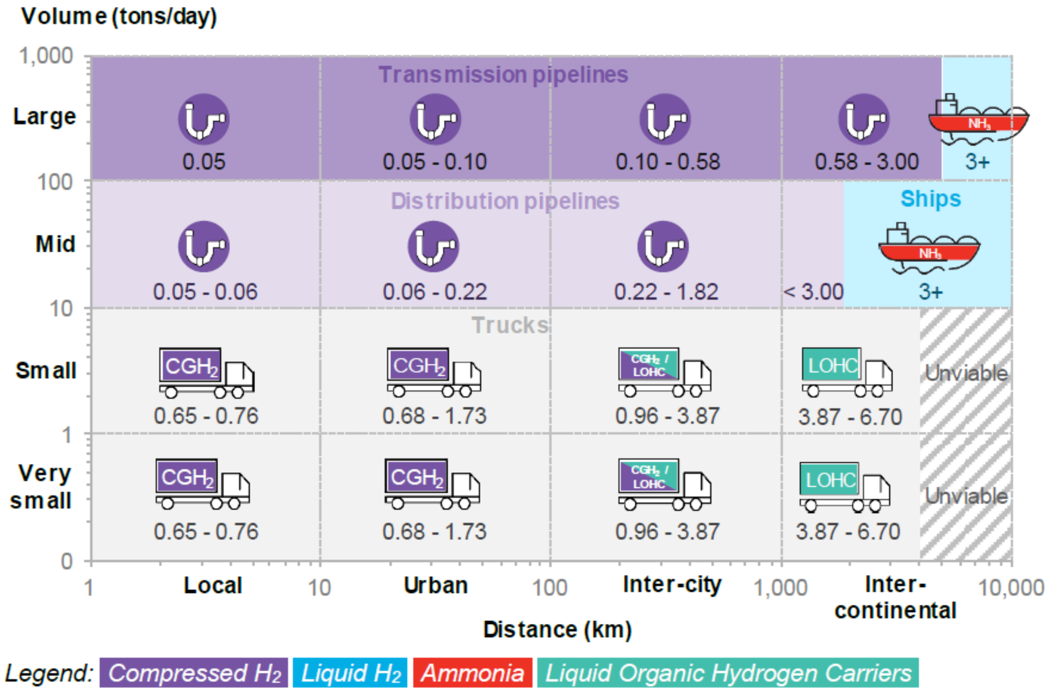

Figure 2-6: Hydrogen transport costs based on the distance and volume [$/kg] [31]

Transport methods [1]:

- **Road transport:** Hydrogen is transported in tanks on trucks in a liquid or compressed state. A truck can transport up to 4,300 kg of LH_2 and up to 360 kg of CGH_2. In the case of CGH_2, losses in the production, distribution, and sales chain are around 4%. Besides, in the tanks' decompression, a small amount remains inside [32].
- **Rail transport:** Tanks have a capacity of 2,900 – 9,100 kg.

- **Sea transport**: Hydrogen, in form of ammonia, is transported in tanks of up to 70 tonnes.
- **Gas pipelines:** By adapting the existing infrastructure, CGH_2 could be transported via existing pipelines.
- **H_2 pipelines:** A new pipeline network would have to be installed for the transport of CGH_2, which would also require large investments. It is similar to the gas system, although due to pressure losses the hydrogen has to be recompressed every 100 km [32].

3 METHODOLOGY

This section presents the methodology carried out in the project, beginning with the electrolyser analysis that has been the starting point for the wind farm design. To this end, the wind resource at the locations of interest, the use of different turbine models, and the system cost have been studied. Next, the possible offshore installation of the electrolyser has been analysed, in addition to the real hydrogen production, energy transport methods, and cost. Thus, obtaining the hydrogen and electricity production, as well as its LCOE. Finally, a sensitivity analysis has been carried out to determine the results reliability and which variables dominate and, therefore, mainly affect the system design (Figure 3-1):

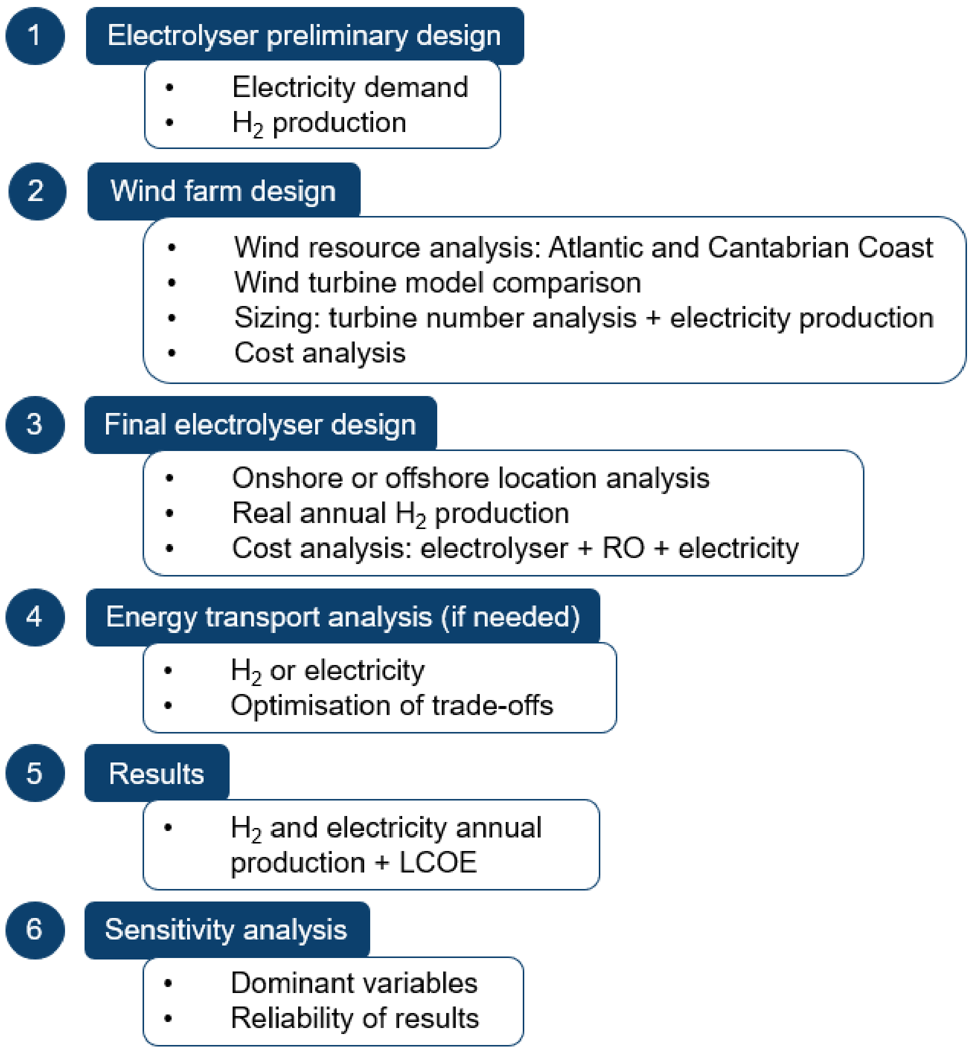

Figure 3-1: Overview of the methodology followed in the project

3.1 Preliminary design of the electrolyser

A first estimation of the energy consumption and the amount of H_2 produced by a 50 MW electrolyser has been performed, comparing the alkaline and the proton exchange membrane (PEM) electrolysers. Table 3-1 and Table 3-2 show the data used in the calculations:

Table 3-1: Technical data of the alkaline and PEM electrolysers [33], [34]

	Alkaline	PEM
CAPEX [€/kWe]	480	700
OPEX [% CAPEX/year]	3	3
OPEX stack replacement [€/kWe]	270	250
Stack lifetime [h]	100,000	90,000
System lifetime [years]	20	20
Electrical efficiency [%, LHV]	68	65.5
Electrical efficiency [kWh/kg]	49.9	51.8

Table 3-2: Baseline data [33], [35]

Electricity price [€/MWh]	165.5
AC/DC converter efficiency [-]	0.95
Obligatory stops [%]	8
Maximum operating hours [h]	8,147

The H_2 production is calculated by the equation (3-1):

$$H_2production = \frac{Efficiency\ (LHV) * Power}{LHV_{H_2}} \tag{3-1}$$

Where $H_2production$ is the H_2 produced by the electrolyser in kg/h, $Efficiency\ (LHV)$ is the electrolyser efficiency to the low heating value, $Power$ is the electrolyser nominal power and LHV_{H_2} is hydrogen's low heating value

(33.93 kWh/kg). The annual H_2 production is obtained by multiplying the hourly production by the annual operating hours of the electrolyser.

The electrolyser annual energy demand is calculated following the equation (3-2):

$$Electricity\ demand = \frac{Operating\ hours * Power}{AC/DC\ efficiency} \quad \textbf{(3-2)}$$

Where $Operating\ hours$ is the number of hours per year the electrolyser is working and $AC/DC\ efficiency$ is the rectifier's efficiency, as the electrolyser operates on direct current and the electricity supplied by the grid is alternating current.

3.2 Wind resource analysis

Section 2.2.1 defines the criteria to be met for an area to be considered suitable for the deployment of a wind farm. Considering these premises, two possible locations are proposed, one in Galicia (Atlantic Coast) and the other on the Cantabrian Coast, near Bilbao.

The advantage of the former is that it has greater wind potential, while the latter despite having a scarcer wind resource, offers the advantage of being located close to the final hydrogen consumption location, the Petronor refinery. Figure 3-2 shows the possible location of the wind farm and Table 3-3 shows their distance to the shore.

Table 3-3: Distance to the shore of the wind farms [36]

Location	Distance to the shore [km]
Galicia	38.93
Bilbao	29.01

Figure 3-2: Location of the wind farm in Galicia and Bilbao [36]

Data provided by the Puertos del Estado model, owned by the Spanish Government [37], are available to study the available wind resource. The closest model points to the previously defined locations have been identified and their characteristics are shown in Table 3-4 :

Table 3-4: Information on the chosen model points [37]

Location	Model code	Longitude	Latitude
Galicia	SIMAR 3032048	8.17º O	44.00º N
Bilbao	SIMAR 3155039	3.04º O	43.63º N

The model provided by Puertos del Estado [37], offers the hourly distribution of wind speed at a 10 m height above sea level. To study the suitability of the wind resource for the deployment of a wind farm, the distribution of wind speeds at the hub height is needed (around 100 m above sea level). For this purpose, equation (3-3), known as the Hellmann exponential law, which relates the wind speed at different heights is used [38].

$$V = V_0 * \left(\frac{Z}{Z_0}\right)^n \quad \textbf{(3-3)}$$

Where V is the wind speed at height Z, V_0 is the wind speed at the height Z_0 and n is a coefficient for correcting the roughness of the terrain. For offshore locations, it ranges from 0.1 to 0.13 [38], [39]. Applying this equation and the data provided by Puertos del Estado [37], the seasonal and annual wind speed distribution for both locations is obtained.

The wind is defined by its speed and direction. The wind turbines are positioned in the direction of the prevailing wind, making maximum use of the available wind resource. Figure 3-3 and Figure 3-4 show the wind rose for SIMAR 3032048 and SIMAR 3155039 points respectively.

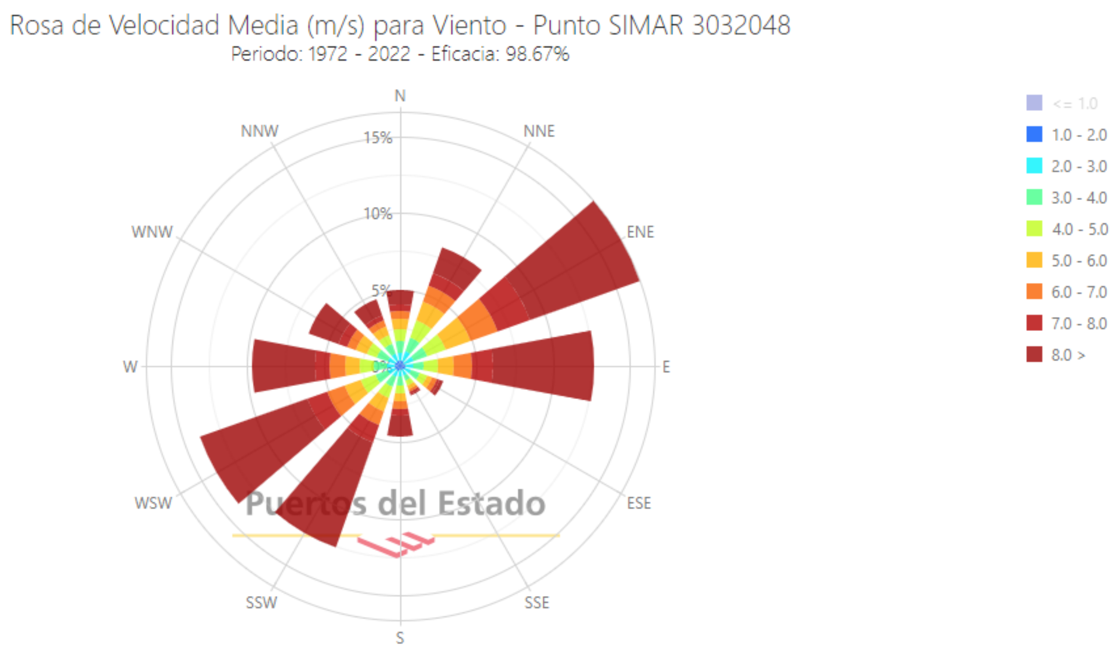

Figure 3-3: Wind rose of point SIMAR 3032048 [37]

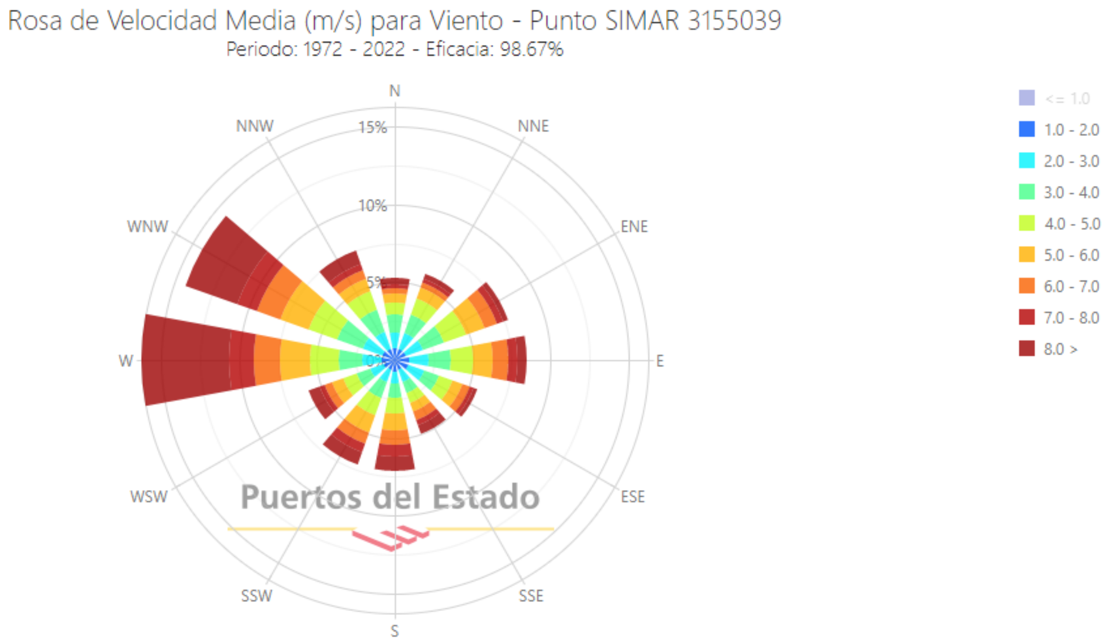

Figure 3-4: Wind rose of point SIMAR 3155039 [37]

From Figure 3-3 it can be seen that the main wind directions are ENE and WSW, with ENE being dominant. In the second case, it is clear that the predominant wind direction is from the west. These directions must be considered when selecting the wind turbines' orientation.

3.3 Comparison of different wind turbine models

In order to analyse the suitability of different wind turbines in both locations, four offshore wind turbines with different power ratings have been chosen.

Table 3-5 presents the main characteristics of the selected models and Figure 3-5 shows their power curves.

Table 3-5: Main characteristics of the selected turbine models [40]–[43]

Model	V164/9500	SG 8.0-167 DD	SWT-6.0-154	SWT-4.0-130
Manufacturer	Vestas	Siemens-Gamesa	Siemens-Gamesa	Siemens-Gamesa
Rated power [kW]	9,500	8,000	6,000	4,000
Rotor diameter [m]	164	167	154	130
Wind class	IEC S	IEC S/IB	IEC IA	IEC IB
Swept area [m^2]	21,125	21,904	18,627	13,274
Specific area [m^2/kW]	2.23	2.74	3.11	3.32
Nº of blades	3	3	3	3
Power control	Pitch	Pitch	Pitch	Pitch
Cut-in wind speed [m/s]	3.5	3.5	3.5	2.5
Rated wind speed [m/s]	14	12	13	12
Cut-off wind speed [m/s]	25	25	25	25
Tower height [m]	*	92 *	*	89.5*

*Site-specific

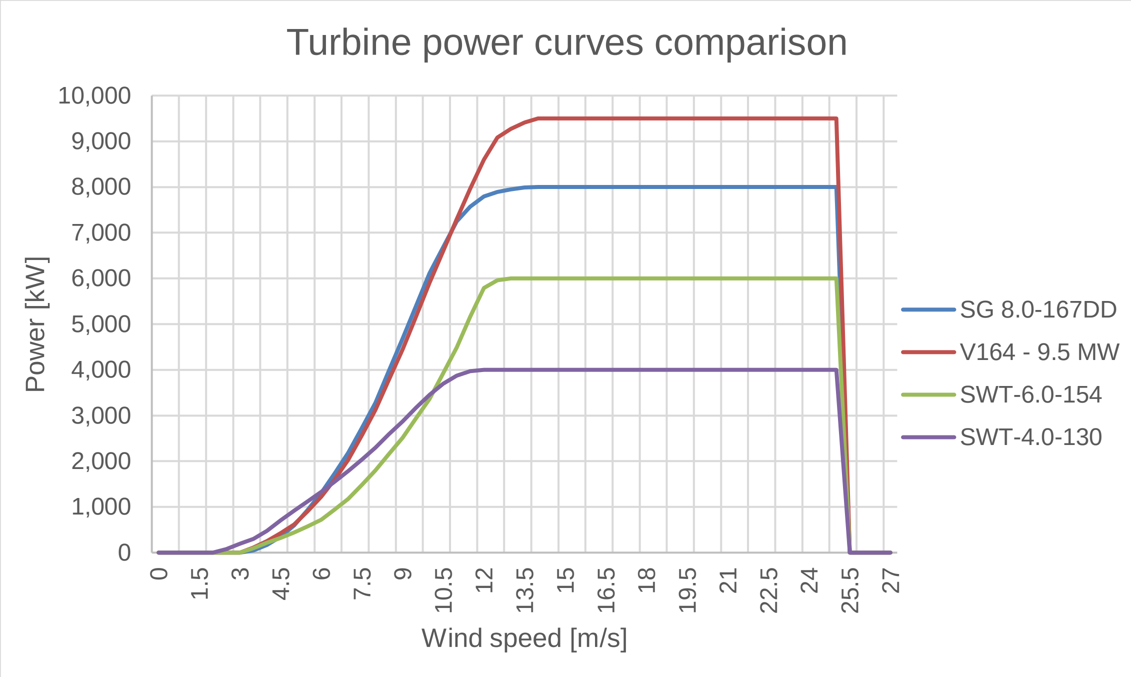

Figure 3-5: Selected turbine models power curves comparison [44]–[47]

The power curves of the V164-9.5 and SG 8.0-167DD models are very similar in the wind speed-dependent curve section, but the former achieves 1.5 MW more rated power than the latter. The 6 MW rated power turbine generates less power than the two previous turbines for any wind speed. Finally, the SWT-4.0-130 model has a lower cut-in speed than the other models, which allows the turbine to produce power at lower speeds.

3.3.1 Energy production

The energy produced annually by the wind turbine is obtained by the distribution of the wind speed at the location and the wind turbine's power curve. Thus, knowing the hourly wind speed distribution, the power curve of the wind turbine is used to obtain the power generated by the wind turbine at any given time.

3.3.2 Capacity factor

The capacity factor of an energy generation system is defined as the ratio between the energy generated and the energy that would have been produced if the power plant had been operating at full load for a specific period of time (3-4):

$$C_p = \frac{Real\ output}{Possible\ maximum\ output} = \frac{Real\ output}{Nominal\ capacity * Hours\ per\ year} \quad \textbf{(3-4)}$$

New offshore wind farms' capacity factors range from 40% to 50% [18], which is much lower than the electrolysers' capacity factor (around 95%, reduced only by the availability factor due to maintenance). This means that for the wind farm to generate the electricity demanded annually by the electrolyser, its power rating must be higher than that of the electrolyser.

3.4 Initial sizing of the wind farm

Knowing the electrolyser annual energy demand and the energy produced by each wind turbine, it is calculated the number of wind turbines that should compose the wind farm to ensure that the energy produced by the wind farm is equal to the energy demanded by the electrolyser. Four wind farm designs are obtained, one for each turbine model. It has also been assumed that the wake phenomenon reduces the annual wind farm electricity production by 3% [48]. This effect occurs because the turbines in the front rows shade the turbines in the rear rows, as well as modify the wind characteristics.

Depending on the year season, the distribution of wind speeds at the site is different, which means that the electricity production is not uniform and, therefore, the electrolyser does not operate for the expected number of hours, nor always at full load. Thus, the energy storage requirement can be determined in each case as the difference between the energy demanded by the electrolyser and the energy produced by the wind farm.

3.5 Analysis of electricity and hydrogen production

The annual electricity produced by the wind farm has been calculated, however, as already mentioned, the energy production is not constant. There are valleys when the wind energy production is lower than the electrolyser demand, and there are peaks when the energy produced is higher than the required by the electrolyser.

For the calculation of the annual hydrogen production and the electricity excess, it has been assumed that the electrolyser has the efficiency shown in Table 3-1 and the operating range shown in Table 3-6:

Table 3-6: Operating range of the electrolyser [33], [34]

	Alkaline	**PEM**
Operating range [%]	10-100	0-100

Therefore, for the alkaline electrolyser, if the energy produced by the wind farm does not exceed 10% of its maximum capacity, it will not operate and the electricity produced in this situation will be considered excess.

In addition, it has been considered that 2% [49] of the electricity produced by the wind farm is lost in the electricity transmission process.

Applying these considerations, the hydrogen and excess electricity produced by each wind farm are calculated for both types of electrolysers.

3.6 Wind farm design analysis, turbine number modification

This section studies the effect that increasing or decreasing the number of turbines that constitute the wind farm would have on both hydrogen production and excess electrical energy. If the wind farm has a higher number of turbines than the number calculated as ideal, the electrolyser will be operating for more hours and at a higher load, however, this will also result in a greater surplus of electricity.

On the contrary, if the number of turbines is reduced, less electrical energy will be available for the operation of the electrolyser, but the excess will also be reduced, providing a better adjustment in case the excess electricity is not used for other purposes.

To carry out this analysis, the number of wind turbines per wind farm has been reduced and increased by four, obtaining for each case the hydrogen and electricity production following the procedure shown in Section 3.5.

3.7 Wind farm cost calculation

3.7.1 CAPEX

Capital expenditures are the costs before the operation of an energy generation plant. It includes the costs associated with environmental studies, development and consenting, turbines and floating platforms, mooring, electricity transmission system, as well as the installation and decommissioning costs of the facility. However, the costs related to the financing of the project itself have not been included.

- **Development and consenting:**

It includes environmental and seabed surveys, project management, and development services. A cost of 210 k€/MW has been estimated for these services [21].

- **Turbines and substructures:**

In floating offshore wind farms, it can be assumed that the turbines cost 1.6 M€/MW [21] and, unlike for fixed offshore technology, the cost of the floating platform on which the turbine is supported is independent of the water depth.

It has been assumed that the WindFloat [50] semi-submersible platform will be used, as it is suitable for supporting 3 to 10 MW turbines at water depths greater than 40 m [51]. The cost per turbine of this type of semi-submersible platform is around 8 M€ [21].

- **Mooring:**

The WindFloat platform has 4 catenary mooring lines, each connected to an anchor [51]. Drag Embedment Anchors, used in this project, are the most commonly used model and cost 123 k€/anchor [51].

Mooring lines are made of steel wire and chain. The length of the lines depends mainly on the site depth. Considering that for a 100 m deep location a 500 m line is needed and that for every 100 m the depth increases, 150 m more line is needed, the line length can be determined. In addition, an extra 60 m has been considered to cope with draught differences [51]. The length of the line follows the equation (3-5):

$$L_{line} = 1.5 * Depth + 410 \quad \textbf{(3-5)}$$

To increase friction and ensure long-term contact with the seabed, 50 m of the chain is used in each mooring line, at 270 €/m [21].

Thus, equation (3-6) is used to calculate the mooring costs for each WindFloat platform:

$$C_{mooring} = n_{lines} * (C_{anchor} + L_{line} * C_{line} + 50 * C_{chain}) \quad \textbf{(3-6)}$$

Where n_{lines} are the number of mooring lines per platform, C_{anchor} is the anchor cost and C_{line} and C_{chain} are the line and chain costs, respectively. The unit cost of the line is 48 €/m [21].

Multiplying this result by the total number of turbines that make up the wind farm the total mooring costs are obtained.

- **Electricity transmission:**

The transmission of electricity to shore is carried out by the following steps: the power generated by the turbine, of around 1 kV, is increased to 33 kV [52] by a transformer located in the nacelle. The electricity is then transmitted to an offshore substation where its voltage is raised (115 kV [49]) and from where the electricity is exported to shore. The cost of the offshore platform is around 39 M€ [21].

The inter-array cable connects the turbines in the same row and the row to the offshore platform. Therefore, the length of the cable to be used depends on the layout of the wind farm, i.e. the number of turbines, the spacing between turbines, and the number of turbines per row.

Optimising the wind farm is a complex process, for simplicity it has been assumed that the turbines are evenly distributed in rows of 5 to 7 turbines [21], [49]. The distance between turbines in the same row has been set at 5 times the rotor diameter [53], while the distance between rows has been estimated at

7 times the rotor diameter [54]. Therefore, a compromise is sought between the reduction of the wake effect and the excessive increase of the transmission lines' cost. In addition, an extra length of 400 m has been considered for each turbine connection [52]. The length of the linking of each row of turbines to the substation has been estimated at 4 km [49].

Based on these considerations and assuming that the cost of inter-array cable is 148.98 k€/km [49], the cabling cost is obtained.

The export of electricity from the offshore substation to land is carried out by a high voltage alternating current (HVAC) cable, which is suitable when the distance to the coast is less than 56 km [21], which is the case of the wind farm to be designed. For longer distances, the use of high-voltage direct current (HVDC) is suggested, as the power losses are lower [21]. The unit cost of the export cable has been estimated at 236.2 k€/km [49].

- **Installation:**

The costs related to the installation of offshore wind farms have a high degree of variability due to the early stage of development, which will allow for significant cost reductions in the future [21]. Installation costs can be divided into turbines, mooring, and electrical infrastructure, which is further divided into inter-array cables, substation, and export cable installation.

For the installation of the turbines it has been assumed that a tug boat is used and that the installation cost per turbine follows the equation (3-7) [21]:

$$C_{installation\_turbine} = \left(T_{install} + 2 * \frac{d_{shore}}{V_{boat}}\right) * \frac{C_{boat}}{n_{turbine\_trip}} \tag{3-7}$$

Where $T_{install}$ is the turbine installation time, d_{shore} is the distance to the coast, V_{boat} is the tug boat's average speed, C_{boat} is the tug boat cost and $n_{turbine\_trip}$ is the number of turbines that can be transported on each trip. The values of these parameters are shown in Table 3-7:

Table 3-7: Turbines installation costs parameters [21]

$T_{install}$ **[days]**	2
V_{boat} **[km/h]**	20
C_{boat} **[k€/days]**	19.5
$n_{turbine\_trip}$ **[-]**	5

The installation cost of the mooring lines has been estimated at 240 k€/turbine [51].

The unit costs associated with the installation of the electricity infrastructure are shown in Table 3-8. By multiplying the total length of the cable by its unit cost, the cabling installation cost is obtained.

Table 3-8: Electrical infrastructure installation costs parameters [21], [52]

Export cable [k€/km]	400
Inter-array cable [k€/km]	190
Substation [M€]	20

- **Decommissioning:**

Although offshore wind projects' decommissioning has not been carried out to date, its cost must be estimated. Onshore wind farm decommissioning costs are insignificant, due to the high return value of scrap metal [21], however, offshore operations and maritime transport imply higher costs. Some studies show that the value of scrap could offset the decommissioning cost [52], but since the value of scrap is highly variable, a decommissioning cost of around 5% of CAPEX is estimated in this project [21].

3.7.2 OPEX

Due to the lack of large-scale floating offshore projects, it is difficult to accurately estimate O&M costs, although they could be around 25% of the total life cycle costs [55]. According to Ref. [52], a floating offshore wind farm located 200 km from the shore would have an annual O&M cost of 131 k€/MW. However, the wind farm under study is located at a shorter distance, and therefore this value has been recalculated and estimated at 70 k€/MW, accounting for around 25% of the farm's costs. In addition, a variable component dependent on the distance to the coast of 40 €/MW*km*year has been considered [21].

3.7.3 Electricity LCOE calculation

The levelized cost of energy is the current cost of developing and operating a power generation facility over its lifetime. For this purpose, the total lifetime costs are calculated and divided by the total energy production (equation (3-8) [56]).

$$LCOE = \frac{\sum_{i=1}^{n} \frac{CAPEX_i + OPEX_i}{(1+r)^i}}{\sum_{i=1}^{n} \frac{E_i}{(1+r)^i}} \tag{3-8}$$

Where $CAPEX_i$ is the initial cost of investment expenditures, $OPEX_i$ is the maintenance and operations expenditures, E_i is the energy generated, r is the project discount rate and n is the system lifetime. The discount rate ranges from 8 to 12% [21] for offshore wind projects, and an intermediate value of 10% has been assumed. The wind farm lifetime has been set at 20 years.

3.8 Hydrogen production cost calculation

This section analyses the cost of onshore and offshore green H_2 production. It has been assumed that the electrolyser cost is the same regardless of whether it is located. Furthermore, in both cases, seawater is used in the process, so it must first be desalinated by a reverse osmosis process. The offshore H_2 production implies a series of additional costs such as H_2 transport to land or the construction and operation of the offshore platform. However, the on-land construction cost is avoided. This procedure allows for deciding which solution is more cost-effective today.

3.8.1 Reverse osmosis

Reverse osmosis seawater desalination has developed rapidly over the last 20 years. The optimisation and improvement in the efficiency of the devices have reduced their energy demand, as well as the CAPEX and O&M costs. This leads to a reduction in the levelized cost of desalinated water, reaching 0.6 $/m^3 [27]. Known that an electrolyser requires approximately 10 kg of water for every kg of H_2 produced, the water demand is estimated, as well as its desalination cost.

Currently, a reverse osmosis plant requires 3 kWh per m^3 of desalinated water [27], knowing the electrolyser water demand, the energy consumption of the desalination plant is calculated.

3.8.2 Compressor

If the pressure at which hydrogen is produced and the supply pressure are different, a compressor is required to raise the pressure. Moreover, if hydrogen is produced offshore, the pressure must be increased to make transport possible. The compressor energy demand is calculated by equation (3-9) [57]:

$$W_{compressor} = \frac{n * R * T * ln\left(\frac{P_2}{P_1}\right)}{\eta} \quad \textbf{(3-9)}$$

Where n is the molar flow of hydrogen, R is the universal gas constant (8.314 J/mol*K), η is the compressor efficiency and P_1 and P_2 are the compressor inlet and outlet pressures.

Usually, the compressor efficiency is close to 70%, however, as it will be working at a variable load, an efficiency of 50% has been considered [57], [58].

Table 3-9 shows the compressor inlet and outlet pressure for each possible scenario. It has been assumed that if the electrolyser is onshore, the compressor raises the output of the alkaline electrolyser to that of the PEM.

Table 3-9: Compressor inlet and outlet pressure [27], [58]

	Onshore		Offshore	
	Alkaline	PEM	Alkaline	PEM
P_1 [bar]	30	50	30	50
P_2 [bar]	50	50	75	75

The cost of the compressor has been assumed to be 10% of the total CAPEX of the electrolyser [59], so it depends on the type of electrolyser.

3.8.3 Offshore H_2 production costs

There are some extra costs due to offshore hydrogen production. It requires the construction of a platform containing the necessary equipment and a transportation method to bring the hydrogen to shore.

- **Offshore platform:**

Based on the literature [57], it has been estimated that the offshore platform is 2.5 times the size of the conventional platform designed for the wind farm and, therefore, its cost has also been assumed to be 2.5 times higher (97.5 M€).

- **H_2 transport:**

According to Figure 2-6, the most appropriate method for transporting H_2 to the shore is by pipelines, which is also a common solution used by Oil & Gas companies to transport gas [57]. In a simplified way, it can be assumed that the unit cost of the pipeline will be 474.3 k€/km [57].

3.8.4 Onshore H_2 production costs

The only additional cost of installing the electrolyser on land is its construction. Civil works usually account for around 24% of the CAPEX of the electrolyser and include tasks such as foundation work, lighting, and building construction [59].

By comparing the offshore and onshore H_2 production costs, the most appropriate solution is determined.

3.8.5 Hydrogen LCOE calculation

The hydrogen cost calculation can be broken down into 3 sections: electrolyser, electricity, and seawater desalination cost.

Reverse osmosis seawater desalination costs 0.006 €/kg H_2 [27] and the cost of electricity consumed by the electrolyser, per hydrogen kg, is calculated using equation (3-10):

$$Electricity\ cost = \frac{Electricity\ LCOE * Electrolyser\ efficiency}{AC/DC\ efficiency} \tag{3-10}$$

Where $Electricity\ LCOE$ is the electricity cost, $Electrolyser\ efficiency$ is the electrolyser efficiency and $AC/DC\ efficiency$ is the rectifier efficiency.

The cost of the electrolyser is further divided into CAPEX and OPEX (Table 3-1). The method for calculating the annual H_2 production has been defined in Section 3.5. Therefore, knowing the electrolyser cost and its production, equation (3-8) is applied to obtain the unit cost of the hydrogen produced. To this result, the cost of electricity consumption and water desalination is added, obtaining the hydrogen LCOE.

3.9 Analysis of energy transport from generation to consumption

If electricity is produced at the wind farm located in Galicia, it has to be defined how the energy will be transported to the consumption place at Petronor, approximately 500 km away.

The energy could be transported to Petronor as electricity, where an electrolyser would produce hydrogen, or it could be produced in Galicia and then transported. The approximate cost of both solutions has been calculated based on previously constructed transmission lines (electricity or hydrogen) in each case.

3.9.1 Electricity transport

In long distances, the transport of electricity can be carried out by HVAC or HVDC systems, as already seen in Section 3.7.1. The cost of electricity transmission substantially increases when substations are needed.

In the use of HVAC cable, it may be necessary to increase the electricity voltage for transport and then reduce it, so it can be used in the electrolyser. The cost of these substations has been assumed to be 27.02 M€ [60]. As regards the cost of the HVAC transmission lines, a wide range of values is available, from 214.4 k€/km to 740.9 k€/km (230 kV) [60], [61]. An intermediate value of 477.66 k€/km has been assumed for the calculations.

If HVDC cables are used, in addition to the voltage changes, an AC/DC conversion of the wind farm electricity has to be undertaken. The cost of the substations varies between 169 and 78 M€ [21], [60], and an intermediate cost of 125 M€ has been established. The cost of HVDC lines ranges between 77.5 k€/km and 407.5 k€/km (400 kV) [60], [61], and an average value of 250 k€/km has been used.

In addition to the system cost, it is crucial to consider the electricity losses of each technology. Figure 3-6 shows the total power losses of HVAC and HVDC transmission:

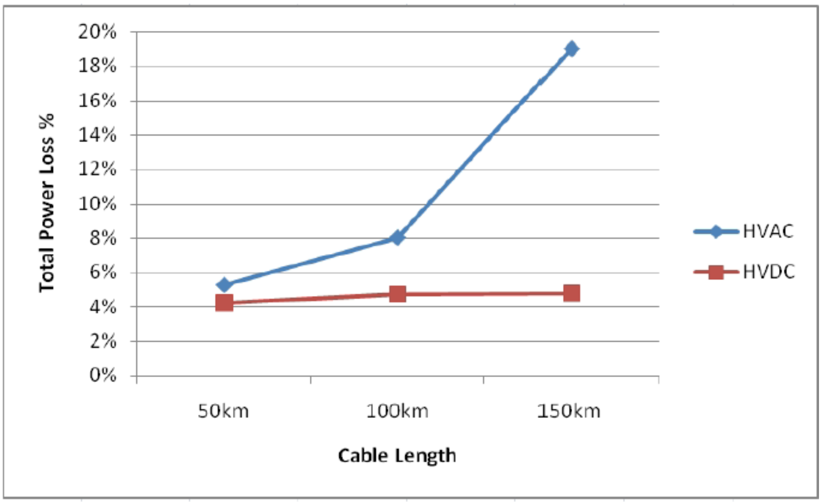

Figure 3-6: Total power loss of HVAC and HVDC transmission systems of a 117 MW plant [62]

As can be seen, the HVAC system losses are much higher than those of HVDC. Moreover, this difference increases with the cable length. It has been assumed that the HVAC transmission losses are 19% and 5% for HVDC transmission.

3.9.2 Hydrogen transport

According to Figure 2-6, considering the electrolyser hydrogen production and the distance to be transported (500 km), pipelines are the most suitable transport method.

The pressure of hydrogen transport pipelines ranges from 10 to 300 bar [57], [63] and the installation cost range from 183.77 to 1,104 k€/km [61], [63]. An average value of 531 k€/km has been considered.

O&M costs are mainly due to the compressor’s energy consumption and maintenance [63]. The hydrogen piping cost from the generation to the consumption location ranges from 0.3 to 0.93 €/kg [63]. A cost of 0.6 €/kg has been estimated for the calculations.

It has been considered that energy losses could occur in the process, accounting for 1% of the H_2 produced [63]. Given the cost and energy losses of each transport method, the final hydrogen cost is calculated.

3.10 Sensitivity and risk analysis

Once the system costs have been calculated, it is crucial to analyse the uncertainty and risk associated with these results, obtaining their reliability. This section shows the procedure carried out, starting with a sensitivity analysis of the system costs and ending with the maximum and minimum costs that could be achieved.

3.10.1 Sensitivity analysis

Palisade’s @RISK software [64] has been used to determine the probability of meeting the calculated budget. This software performs Monte Carlo simulations to obtain the probability of occurrence of a given scenario, defining the reliability of the results obtained. It also allows defining the distribution that characterises each budget item and, therefore, its effect on the final result.

The variables that contribute most to the variance of the system have also been analysed. In this way, the wind farm, the electrolyser, and energy transport have been studied separately, to subsequently analyse the implications of each of them on the total cost of the system.

- **Wind farm:**

Table 3-10 shows the unitary costs of the wind farm, from the development and consenting costs to the installation costs of the equipment used.

Table 3-10: Wind farm unitary costs [21], [49], [51], [52]

	Wind farm		
	Minimum	**Mean**	**Maximum**
Development and consenting [k€/MW]	153.30	210.00	252.00
Turbine [M€/MW]	1.28	1.60	1.73
Substructure [M€/turbine]	8.00	8.00	8.00
Mooring [M€/turbine]	0.51	0.68	0.85
Export cable [M€/km]	0.22	0.24	0.53
Offshore platform [M€]	31.20	39.00	50.00
Inter-array cable [k€/km]	140.00	148.98	323.15
Turbine installation [M€/turbine]	0.02	0.02	0.47
Mooring installation [k€/turbine]	192.00	240.00	288.00
Export cable installation [k€/km]	354.00	400.00	826.00
Inter-array cable installation [k€/km]	171.00	190.00	209.00
Offshore platform installation [M€]	18.60	20.00	21.40

The costs have been defined per wind farm power, turbine, or cable length so that knowing the specific characteristics of the wind farm, the total CAPEX is obtained. For simplicity, decommissioning costs have not been considered in this analysis, as studies show that they could be negligible due to steel sales [21], [52].

- **Electrolyser:**

Table 3-11 shows the parameters that define the minimum, mean and maximum costs of the two types of electrolysers studied in this project.

Table 3-11: Alkaline electrolyser unitary costs [1], [33], [34]

	Alkaline		
	Minimum	**Mean**	**Maximum**
CAPEX [€/kWe]	400	480	850
OPEX [% CAPEX/year]	2	3	6
OPEX stack replacement [€/kW]	270	270	270
Electrical efficiency [%, LHV]	71	68	65

Table 3-12: PEM electrolyser unitary costs [1], [33], [34]

	PEM		
	Minimum	**Mean**	**Maximum**
CAPEX [€/kWe]	600	700	1,300
OPEX [% CAPEX/year]	3	3	5
OPEX stack replacement [€/kW]	250	250	250
Electrical efficiency [%, LHV]	68	65.5	63

For this comparison, it has been assumed that the electrolyser has a 20 years lifetime and that the stack will be replaced once in this period. In addition, it has been assumed that both systems will operate for the maximum possible time, 92% capacity factor.

- **Energy transport:**

Table 3-13, Table 3-14, and Table 3-15 show the unit costs that define the CAPEX of transporting energy from the production to the consumption locations, considering the transport of electricity through HVDC land HVAC lines and hydrogen pipelines, respectively.

Table 3-13: HVDC transmission unitary costs [21], [60], [61]

	HVDC transmission line		
	Minimum	**Mean**	**Maximum**
HVDC cable [k€/km]	77.50	250.00	407.50
Substation [M€]	78.00	125.00	169.00

Table 3-14: HVAC transmission unitary costs [60], [61]

	HVAC transmission line		
	Minimum	**Mean**	**Maximum**
HVAC cable [k€/km]	214.40	477.66	740.90
Substation [M€]	22.96	27.02	31.07

Table 3-15: H_2 transmission unitary costs [61], [63]

	H_2 pipeline		
	Minimum	**Mean**	**Maximum**
H_2 pipeline [k€/km]	183.77	531.00	1,104.00

Once the system specifications are known the minimum, the most likely, and maximum cost of each budget item is obtained from the unitary cost.

Knowing these results, the next step is to define the distribution that characterises the behaviour of each variable. @RISK software [64] provides several distribution options, both discrete and continuous. A Pert distribution has been used to define each variable, as this type of distribution is widely used in cost and risk analysis.

Defined the distribution of each budget item, the total budget is determined, which is set as the output of the simulation. Simulating 10,000 iterations, the probability of meeting the estimated budget is obtained, as well as the possible minimum and maximum budget, defined as the results that have a 5% and 95% probability of being met, respectively. The contribution to the variance of each variable has also been calculated.

This procedure has been followed for each system (wind farm, electrolyser, and energy transport), as well as for the whole system.

3.10.2 Comparison of maximum and minimum results

Once the cost uncertainty of each system has been calculated, the most favourable and most unfavourable scenarios have been defined:

- Most favourable: the lowest budget that could be met, assuming a 5% probability of staying in the budget.
- Most unfavourable: the most conservative budget, assuming a 95% probability of being met.

The total minimum and maximum CAPEX of the system are obtained by applying equations (3-11) and (3-12) respectively:

$$\begin{aligned} Total\ CAPEX\ (5\%) &= Wind\ farm\ (5\%) + Electrolyser\ (5\%) \\ &+ Energy\ transport\ (5\%) \end{aligned} \tag{3-11}$$

$$\begin{aligned} Total\ CAPEX\ (95\%) &= Wind\ farm\ (95\%) + Electrolyser\ (95\%) \\ &+ Energy\ transport\ (95\%) \end{aligned} \tag{3-12}$$

Knowing the system CAPEX and the annual electricity and hydrogen production, the LCOE of each product is recalculated. This allows for comparison and validates the results obtained.

4 RESULTS AND DISCUSSION

4.1 Preliminary design of the electrolyser

Based on the characteristics shown in Table 3-1 and Table 3-2 and using equations (3-1) and (3-2), the annual electricity demand, CAPEX, and hydrogen production of a 50 MW alkaline and PEM electrolyser have been obtained.

The energy requirement of both electrolyser types is identical, as it does not depend on the electrolyser efficiency, and has been estimated at 424.17 GWh/year. However, the maximum hydrogen production and the CAPEX does depend on its characteristics, obtaining results shown in Table 4-1:

Table 4-1: Annual maximum hydrogen production and CAPEX

	Alkaline	PEM
H_2 production [tonne/ year]	8,075.83	7,778.92
CAPEX [M€]	24	35

The alkaline electrolyser produces annually 3.7% more than the PEM, so the energy demand of the RO process is also higher, 0.24 and 0.23 GWh, respectively. Table 4-2 shows the annual compressor electricity demand:

Table 4-2: Annual compressor energy demand

	Onshore		Offshore	
	Alkaline	PEM	Alkaline	PEM
Energy demand [GWh/year]	2.70	0.00	4.89	2.08

Although a priori the alkaline electrolyser seems to have better characteristics, calculations have been carried out for both types, as the PEM has the advantage of having a higher operating range and lower compression need.

4.2 Wind farm design

This section shows the results obtained in the wind farm design process. Starting with the wind resource analysis, followed by the annual electricity generation and the capacity factor of different wind turbine models' calculations, as well as the wind farm sizing. The final use of the produced electricity, i.e. whether it is used for hydrogen production or whether, if it is greater than the electrolyser demand, it should be managed or sold to the grid. Finally, the project costs and the electricity LCOE have been defined.

4.2.1 Wind resource analysis

Figure 4-1 and Figure 4-2, show the wind speed distribution on the Atlantic Coast, Galicia, and on the Cantabrian Coast, Bilbao, obtained from data provided by the Spanish Government [37] and applying equation (3-3):

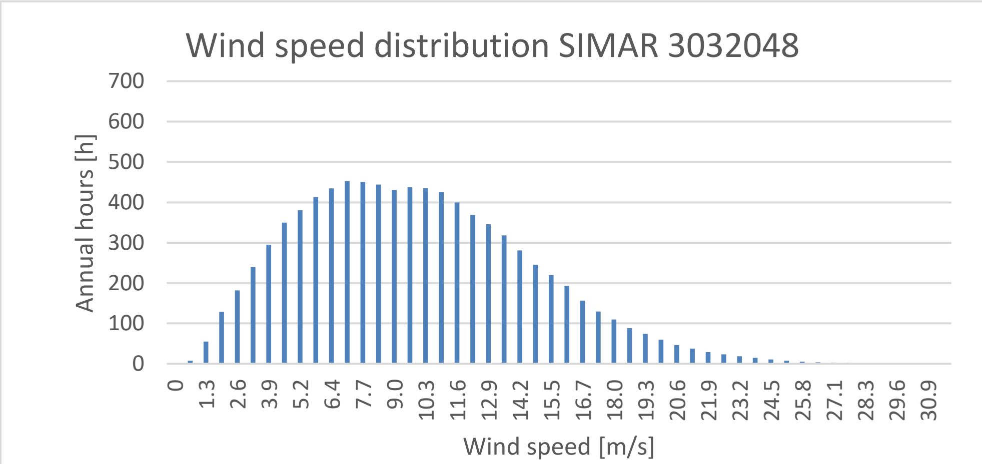

Figure 4-1: Annual wind speed distribution at SIMAR 3032048 point (Atlantic Coast, Galicia) at 100 m above sea level

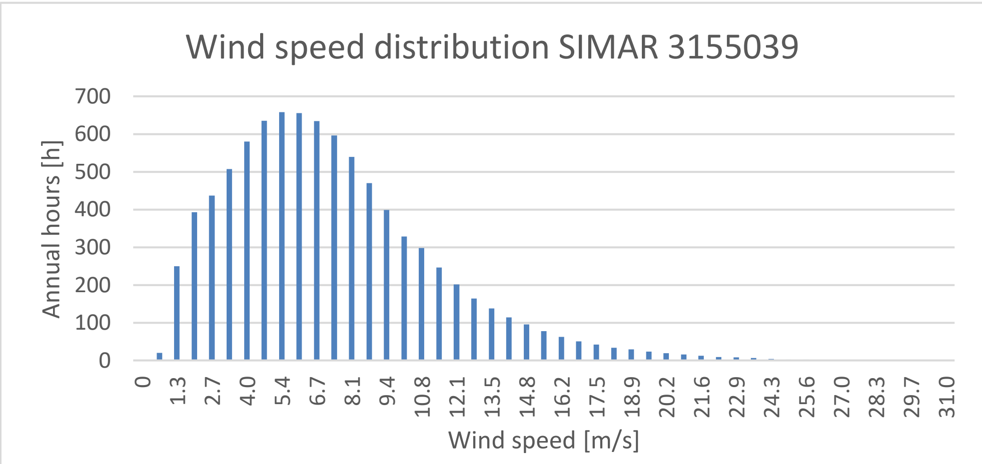

Figure 4-2: Annual wind speed distribution at SIMAR 3155039 point (Cantabrian Coast, Bilbao) at 100 m above sea level

Based on Figure 4-1 and Figure 4-2, the wind speed distribution is more uniform on the Galician coast, accounting for wind speeds between 6 and 16 m/s for 70% of the year and reaching a maximum of 453 hours per year at a wind speed of 7.1 m/s. However, in the second location, the speed distribution is sharper, concentrating on speeds between 4 and 8.1 m/s. These lead to an average wind speed of 9.92 and 7.3 m/s, in each location. Therefore, the Atlantic Coast has a better wind resource than the Cantabrian Coast.

Appendix A shows the distribution of seasonal wind speeds for each site, as the wind resource available depends on the time of the year. It is mainly observed that summer and winter have the lowest and the highest wind resource respectively, being this difference more noticeable on the Cantabrian Coast than on the Atlantic Coast.

4.2.2 Electricity production and capacity factor per turbine

Table 4-3 shows the annual production of the four turbine models described in Section 3.3, while Table 4-4 shows the seasonal distribution of the production.

Table 4-3: Annual electricity generation per turbine

	Annual electricity generation per turbine [GWh]			
Location	V164-9.5	SG8.0-167DD	SWT-6.0-154	SWT-4.0-130
Galicia	43.67	40.23	27.22	22.99
Bilbao	25.25	24.18	13.85	15.65

In both locations V164-9.5 model offers the maximum electricity generation, being 42.2% higher in Galicia. However, the minimum result in Galicia is obtained with the 4 MW turbine, while in Bilbao it is achieved with the SWT-6.0-154 model. This is because the power curve of the SWT-4.0-130 is better adjusted to the wind characteristics in Bilbao, with higher power at low wind speeds.

Table 4-4: Seasonal distribution of electricity production

		Seasonal distribution of electricity production [%]			
Location		V164-9.5	SG8.0-167DD	SWT-6.0-154	SWT-4.0-130
Galicia	Spring	25%	26%	25%	25%
	Summer	20%	21%	20%	22%
	Autumn	25%	25%	25%	25%
	Winter	30%	28%	30%	28%
Bilbao	Spring	26%	26%	26%	26%
	Summer	17%	17%	16%	19%
	Autumn	25%	25%	25%	25%
	Winter	32%	32%	33%	30%

As expected from the seasonal wind speed distribution analysis, the maximum electricity production is obtained in winter and the minimum in summer. Overall, smaller turbines adjust better to resource variations, offering a more uniform production. However, in Bilbao, the 6 MW rated turbine offers a less homogeneous production.

This phenomenon implies the use of energy storage if the electrolyser is required to operate during the estimated design hours. However, in this project, energy storage has not been considered and the final hydrogen production and electricity excess have been estimated in each case.

Table 4-5 shows the capacity factor of each turbine model at both locations:

Table 4-5: Turbine capacity factor

	Turbine capacity factor [%]			
Location	V164-9.5	SG8.0-167DD	SWT-6.0-154	SWT-4.0-130
Galicia	52%	57%	52%	66%
Bilbao	30%	35%	26%	45%

The capacity factor indicates the utilisation of the installation, so a high capacity factor means that the turbines are in operation for a longer time. The highest capacity factor has been obtained with the lowest rated power model, as it requires a lower wind speed to produce electricity.

However, it should be noted that the model SWT-6.0-154, with a rated power of 6 MW, has a low capacity factor. This is due to the shape of its power curve, producing lower power than other models in the speed-dependent part of the curve. Due to the low capacity factor and power output, and the non-uniformity of the output, it has been decided to exclude this model.

4.2.3 Wind farm sizing

Once the electrolyser annual demand and the turbine electricity generation are known, the number of turbines that make up the wind farm is defined. Losses of 3% due to the wake effect have been considered. As expected, fewer turbines are needed when high-quality wind resources and high-power wind turbines are available (Table 4-6).

Table 4-6: Minimum turbine number

	Minimum turbine number		
Location	V164-9.5	SG8.0-167DD	SWT-4.0-130
Galicia	11	12	20
Bilbao	18	19	29

Table 4-7 shows the annual electricity production of each wind farm, considering also the electricity transmission losses.

Table 4-7: Annual electricity generation per wind farm

	Annual electricity generation per wind farm [GWh]		
Location	V164-9.5	SG8.0-167DD	SWT-4.0-130
Galicia	456.38	458.57	436.86
Bilbao	431.81	436.49	431.10

Based on the characteristics of the electrolysers (Table 3-1 and Table 3-6) electricity usage is defined: as hydrogen production or sold to the grid. Figure 4-3 shows the annual hydrogen production of each wind farm comparing the use of PEM and alkaline electrolysers.

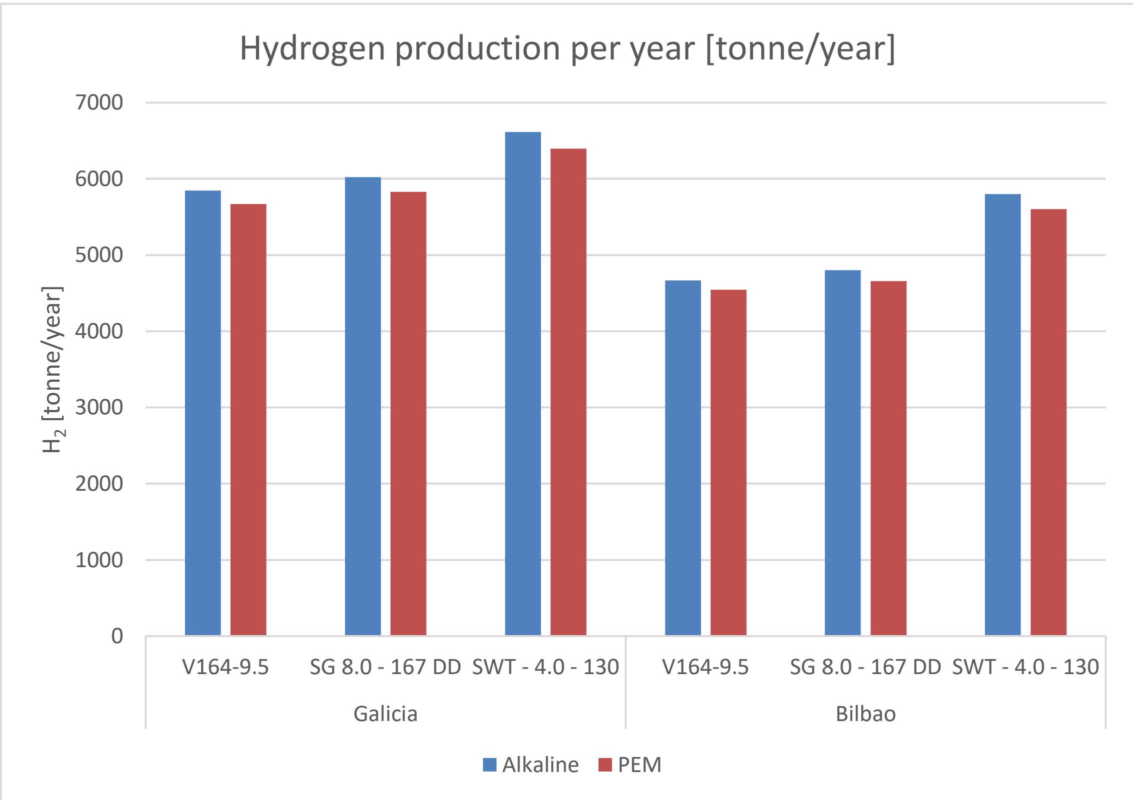

Figure 4-3: Annual hydrogen production

The annual hydrogen production of the alkaline electrolyser is higher than the PEM due to its higher efficiency, even though the operating range is 10% lower. As the PEM cost is higher, an alkaline electrolyser is used in this project.

At both locations, hydrogen production increases when smaller turbines are used, even though the total electricity supplied by the turbines is lower (Table 4-7). This is because at low wind speeds their electricity production is higher, allowing the electrolyser to run for a longer time. Therefore, the electricity produced and not used for hydrogen production is less (Figure 4-4).

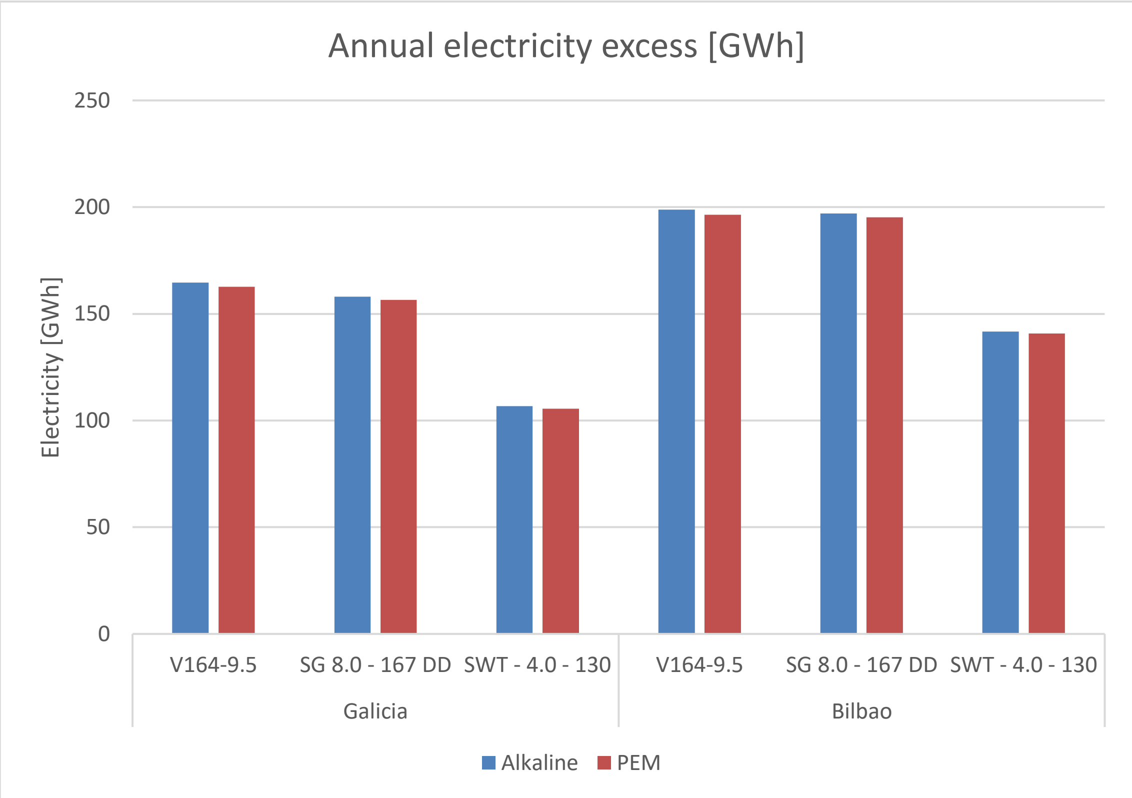

Figure 4-4: Annual electricity excess production

The wind farm that allocates most of its production to hydrogen production is the one located in Galicia and formed by SWT-4.0-130 turbines since only around 24% of the electricity generated is not destined for hydrogen production. In contrast, the least efficient is the 9.5 MW turbine plant in Bilbao, where approximately 46% of the electricity is fed to the grid.

4.2.4 Wind farm turbine number variation effect

From the base case shown above, in which the wind farm is designed to produce the electricity demanded by the electrolyser annually, the effect of increasing and decreasing the number of turbines that make up the wind farm has been analysed. Table 4-8 and Table 4-9 show the number of turbines that would make up the field in each location:

Table 4-8: Number of turbines for each scenario Galicia

	Number of turbines in Galicia		
Scenario	V164-9.5	SG8.0-167DD	SWT-4.0-130
G_-4	7	8	16
G_-3	8	9	17
G_-2	9	10	18
G_-1	10	11	19
G_0	11	12	20
G_1	12	13	21
G_2	13	14	22
G_3	14	15	23
G_4	15	16	24

Table 4-9: Number of turbines for each scenario Bilbao

	Number of turbines in Bilbao		
Scenario	V164-9.5	SG8.0-167DD	SWT-4.0-130
B_-4	14	15	25
B_-3	15	16	26
B_-2	16	17	27
B_-1	17	18	28
B_0	18	19	29
B_1	19	20	30
B_2	20	21	31
B_3	21	22	32
B_4	22	23	33

Following the same procedure as in the reference scenario, the total annual electricity production has been determined, as well as that for hydrogen production and that which is fed into the grid or used for other purposes.

Figure 4-5 shows the electricity use in the possible scenarios in Bilbao, increasing and decreasing by 4 the number of turbines when the V164-9.5 model is used. As can be seen, as the number of wind turbines increases, the total electricity production, the hydrogen production, and, also, the electricity that cannot be used for hydrogen production increase. Furthermore, it is worth noting that while hydrogen production increases slowly, electricity excess increases at a much steeper rate. So that in scenario B_-4, around 64% of the electricity produced is used for hydrogen production, while in B_4, only 47% is used for hydrogen production.

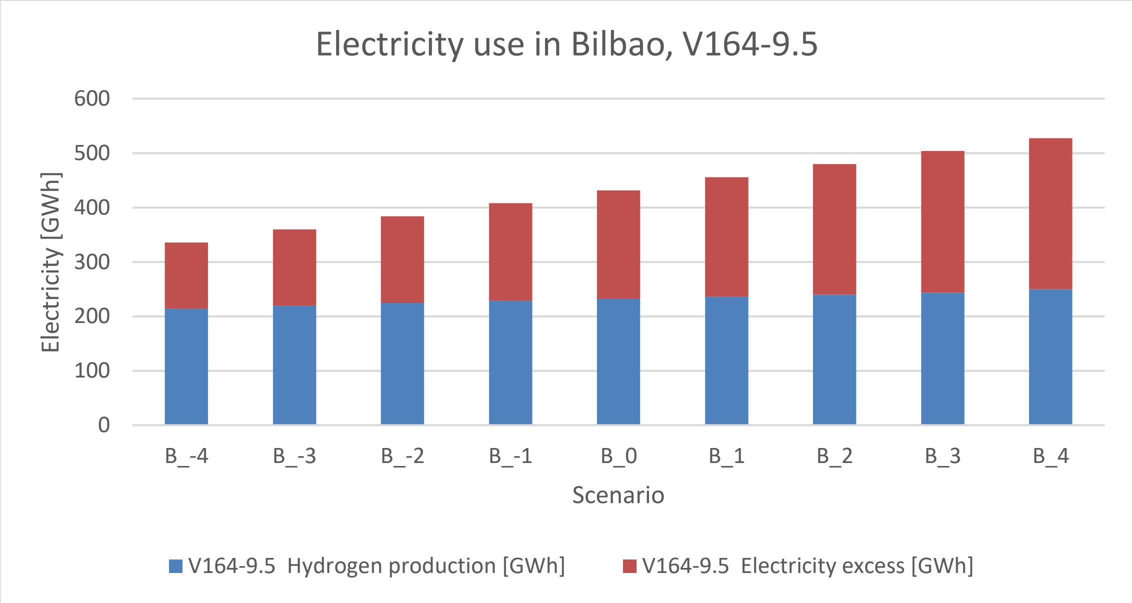

Figure 4-5: Electricity use in the Bilbao scenarios using the V164-9.5 turbine, alkaline electrolyser

Figure 4-6 shows the results obtained for different scenarios using the SWT-4.0-130 model in Galicia. The same trend explained in the previous case is observed: in scenario G_-4, 88% of the electricity is used for hydrogen production, while in G_4 it is reduced to 66%.

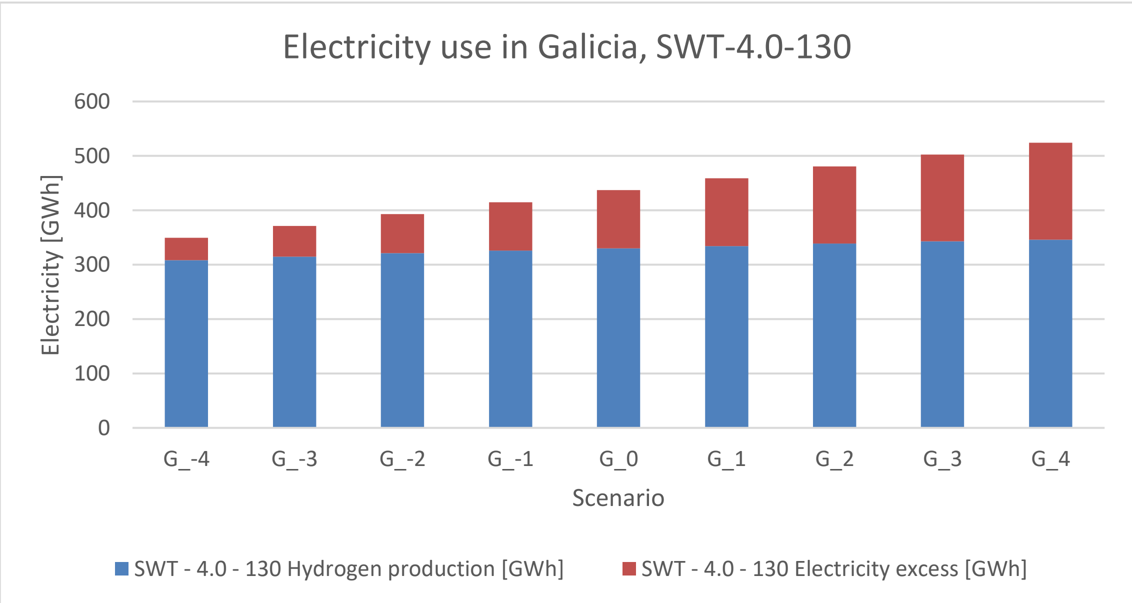

Figure 4-6: Electricity use in the Galicia scenarios using the SWT-4.0-130 turbine, alkaline electrolyser

All the scenarios analysed follow the same trend, so it is necessary to analyse in each case whether, it is more appropriate that most of the electricity is used for hydrogen production or whether it is better to increase the electricity production, with the consequences that this entails. A cost analysis has been carried out to analyse which option is the most economically viable.

4.3 Wind farm cost analysis

4.3.1 CAPEX

The construction, commissioning, and decommissioning costs of the wind farm are presented below.

Table 4-10 shows the development and consenting costs, as well as the equipment cost, per turbine unit. To obtain the total cost, these results have been multiplied by the number of turbines in the wind farm (results in Appendix B).

Table 4-10: Wind farm costs defined per turbine unit

	Cost [M€/turbine]		
Cost type	V164-9.5	SG8.0-167DD	SWT-4.0-130
Development and consenting	2.00	1.68	0.84
Turbine and substructure	23.2	20.8	14.4
Mooring	0.68	0.68	0.68

Mooring costs are identical for the three types of turbines, as the same mooring system has been used. However, the turbines and D&C costs depend on the turbine power. WindFloat platform has been used for the three models, at 8 M€.

Electricity transmission costs are divided into three groups: inter-array cabling, offshore platform, and export cable.

The offshore platform costs 39 M€ and the export cable cost is the same for all scenarios at the same location, as it only depends on the unit cost of the cable and its length (Table 4-11).

Table 4-11: Electricity export cost: export cable and offshore platform

	Cost [M€]	
Cost type	Galicia	Bilbao
Export cable and offshore platform	48.20	45.85

As detailed in Section 3.7.1, the inter-array cabling cost depends on the number and length of connections. Appendix B.4.2 shows the length of the cable used and the total cost. Table 4-12 shows the results obtained for the reference case, i.e. G_0 and B_0:

Table 4-12: Inter-array cabling costs for the reference cases in Galicia and Bilbao, G_0 y B_0

	Inter-array cabling cost [M€]		
Scenario	V164-9.5	SG8.0-167DD	SWT-4.0-130
G_0	2.83	3.03	4.45
B_0	4.51	4.73	6.73

As the number of turbines on the wind farm increases, the inter-array cable cost increases, however, this relationship is not proportional between wind farms composed of different types of turbines, as the spacing between turbines is proportional to the diameter of the turbine rotor. Therefore, smaller turbines require shorter spacing and connection cables.

The installation costs are divided into three main groups: turbines, mooring, and electrical infrastructure as defined in Section 3.7.1. Table 4-13 shows the G_0 and B_0 scenarios' results. The results obtained for the rest of the scenarios are available in Appendix B.

Table 4-13: Total installation cost for the base cases in Galicia and Bilbao, G_0 and B_0

	Total installation cost [M€]		
Scenario	V164-9.5	SG8.0-167DD	SWT-4.0-130
G_0	42.05	42.57	46.46
B_0	42.05	42.59	47.74

The installation costs are very similar in Bilbao and Galicia, as although more turbines are deployed in Bilbao, they are closer to the shore. The electrical installation accounts for around 85% of the installation cost and the offshore platform installation is the most expensive task (20 M€).

Figure 4-7 presents the wind farm CAPEX against the wind farm power in both locations. For the same wind farm capacity, high-rated power turbine wind farms have a lower CAPEX, since they are made up of fewer turbines and therefore, costs that depend on the number of turbines (mooring costs, substructures, and inter-array cabling and their installation) are lower.

It is also observed that for the same installed capacity if the wind farm is located in Galicia, the CAPEX is slightly higher than if it were located in Bilbao. This is because it is further from the shore, increasing the cost of electricity export cable.

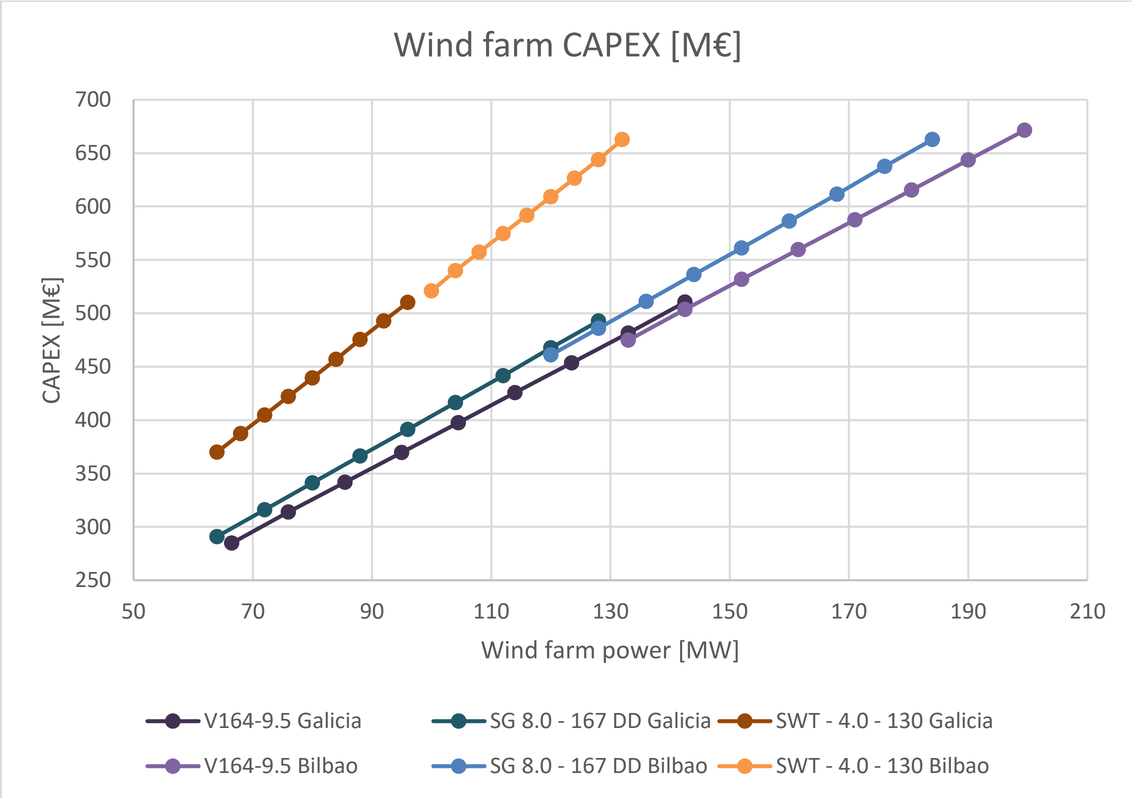

Figure 4-7: Wind farm CAPEX, Galicia and Bilbao

4.3.2 OPEX

The O&M costs of the plant have been defined in proportion to its power output and the distance from the shore, this is why they are slightly higher in Galicia than in Bilbao. Table 4-14 summarises the O&M costs per turbine for each location:

Table 4-14: OPEX per turbine

	OPEX [M€/turbine*year]		
Location	V164-9.5	SG8.0-167DD	SWT-4.0-130
Galicia	0.680	0.572	0.286
Bilbao	0.676	0.569	0.285

4.3.3 Electricity LCOE

Knowing the CAPEX, OPEX, and total electricity production for each scenario, using equation (3-8) the electricity LCOE is calculated for each alternative (Figure 4-8).

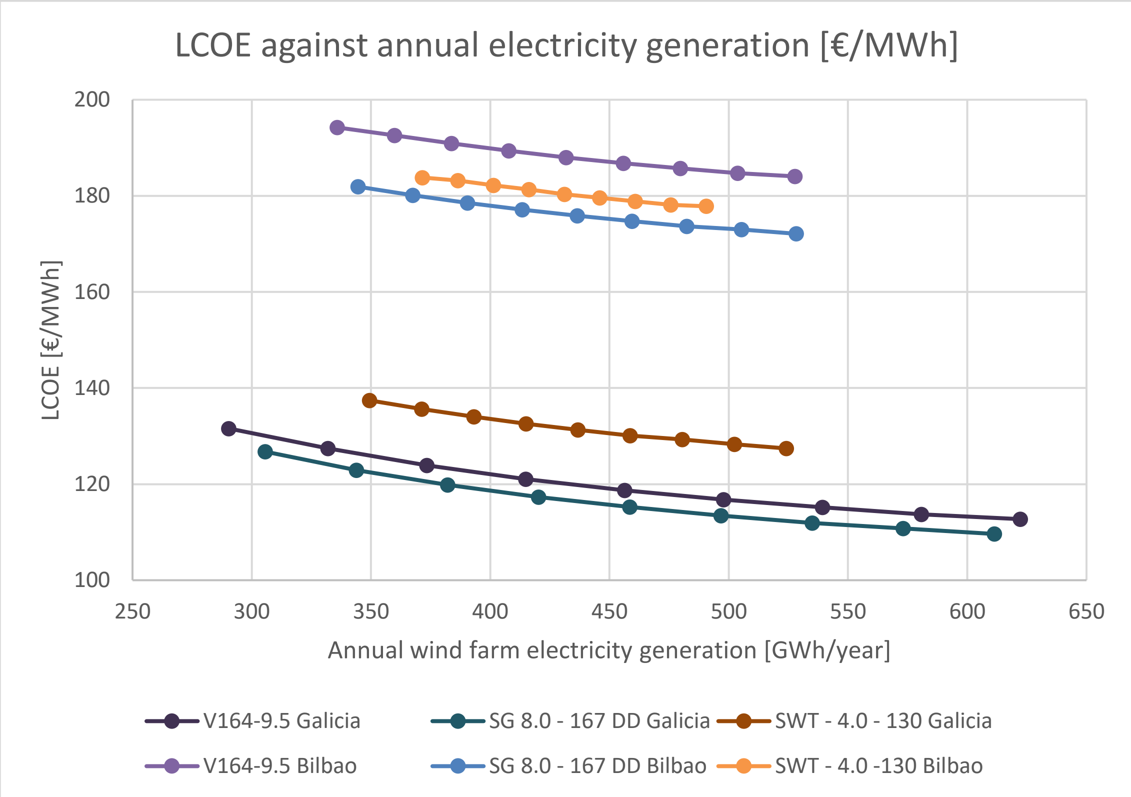

Figure 4-8: LCOE against wind farm electricity generation

The higher the electricity production of the wind farm, i.e. the higher the power output, the lower the electricity LCOE. In both locations the minimum LCOE is obtained using SG 8.0-167 DD turbines, achieving 109.63 €/MWh and 172.10 €/MWh, in Galicia and Bilbao, respectively.

On the other hand, the maximum value is obtained in Bilbao using the V164-95 model, 194.23 €/MWh, while the maximum achieved in Galicia is 137.42 €/MWh (SWT-4.0-130), which is lower than the minimum LCOE in Bilbao.

These results show that large-rated power turbines are more suitable in locations with a high wind resource, while in sites where the wind resource is scarcer, the use of smaller-rated power turbines is more appropriate.

Results obtained for the reference scenario are shown in Table 4-15:

Table 4-15: Electricity LCOE for the reference case, G_0 and B_0

	LCOE [€/MWh]		
Scenario	V164-9.5	SG8.0-167DD	SWT-4.0-130
G_0	118.71	115.21	131.28
B_0	188.01	175.83	180.35

The LCOEs obtained in Galicia are between 20.68% and 30.39% below the considered grid electricity price (165.5 €/MWh [35]), while in Bilbao they are greater (between 6.24% and 13.6%).

4.4 Hydrogen production cost

The costs associated with hydrogen production are mainly divided into three groups: electrolyser, electricity, and reverse osmosis cost. However, if hydrogen is produced offshore, there are additional costs to consider. In a simplified way, the increase in the size of the offshore platform and the hydrogen transport to the consumption location can be considered, although the cost of the onshore construction of the electrolyser has to be discounted. Figure 4-9 shows the total CAPEX of onshore and offshore alkaline electrolyser:

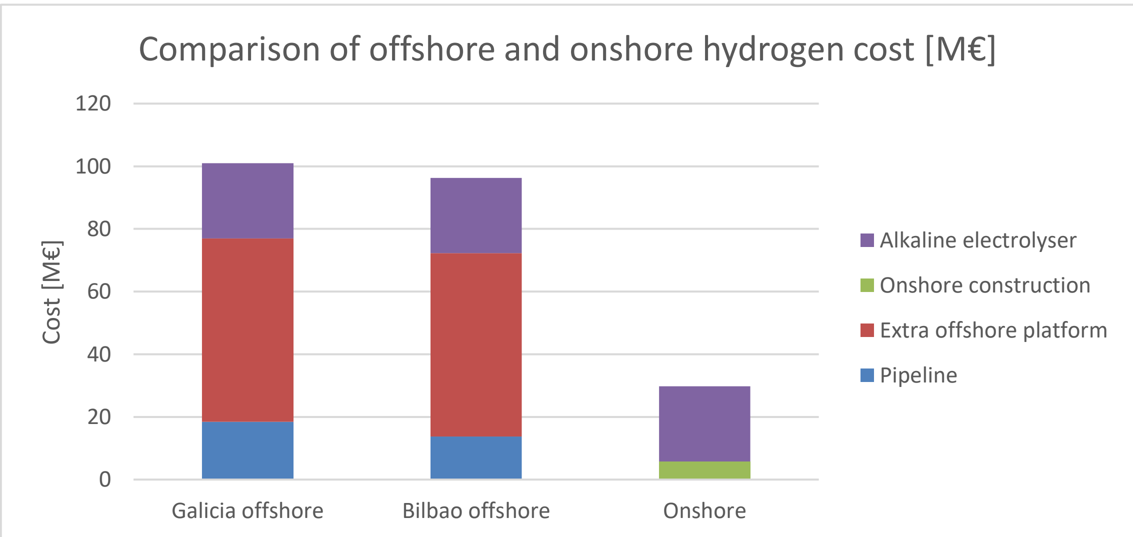

Figure 4-9: Comparison of offshore and onshore H_2 production system CAPEX

The deployment of an offshore facility is much more expensive than onshore, as the cost of the onshore civil work is less than 10% of the offshore platform cost. The pipeline cost depends on the distance to the shore, accounting for 18.3% and 14.3% of the total cost respectively in Galicia and Bilbao.

In addition, a more powerful compressor unit would be required for hydrogen transport, which would further increase the cost, in addition to increased O&M work. For these reasons, with the technology and costs currently available, the onshore installation of the plant has been chosen.

4.4.1 Hydrogen LCOE

Figure 4-10 shows the hydrogen LCOE breakdown for the reference scenarios (G_0 and B_0). For this comparison, it has been considered that hydrogen is generated in an electrolyser that would be located near the coast: in Bilbao, at the consumption site in Petronor, and in Galicia, Atlantic Coast. Therefore, the cost of transporting energy from Galicia to Bilbao has not been considered in this comparison, although it will be defined in the following sections.

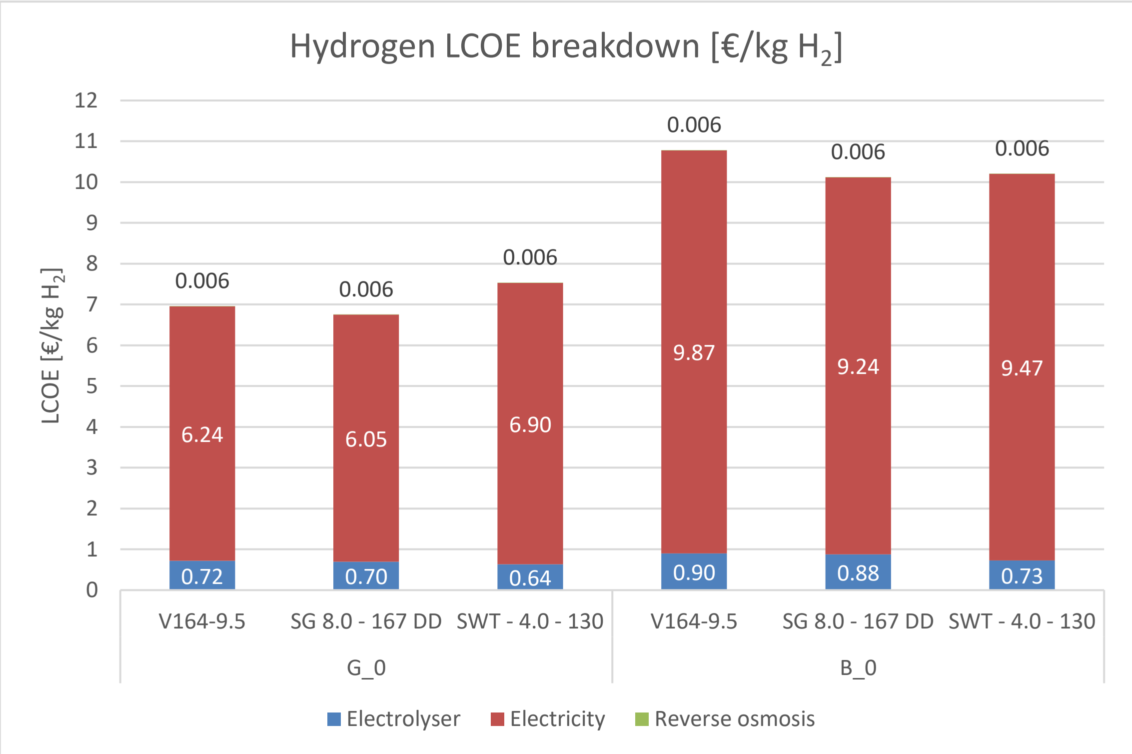

Figure 4-10: Hydrogen LCOE breakdown

The main cost is due to the electrolyser's high electricity consumption and it is, therefore, related to the electricity cost. In the six scenarios shown, this item accounts for around 90% of the hydrogen LCOE. Therefore, reducing the electricity cost has a major impact on the final cost of hydrogen.

Figure 4-11 shows the hydrogen LCOE for all the studied scenarios. For the scenarios in which the wind farm is located in Galicia, without considering the cost of transporting the energy to the hydrogen consumption site.

The minimum LCOE is obtained by situating the wind farm in Galicia and using the SG 8.0-167 DD turbine model, achieving 6.42 €/kg LCOE and reaching a hydrogen production of 6,428.8 tonnes/year. The maximum production is achieved by the wind farm located in Galicia and with 4 MW turbines, generating 6,935.21 tonne/year, at 7.31 €/kg. To these results must be added the energy transporting cost to obtain the hydrogen final LCOE.

If the wind farm is located in Bilbao, the maximum production is also obtained using the SWT-4.0-130 model (6,058.10 tonne/year, 10.04 €/kg), while the lowest LCOE is achieved using the SG8.0-167DD turbine (5,095.30 tonne/year, 9.87 €/kg).

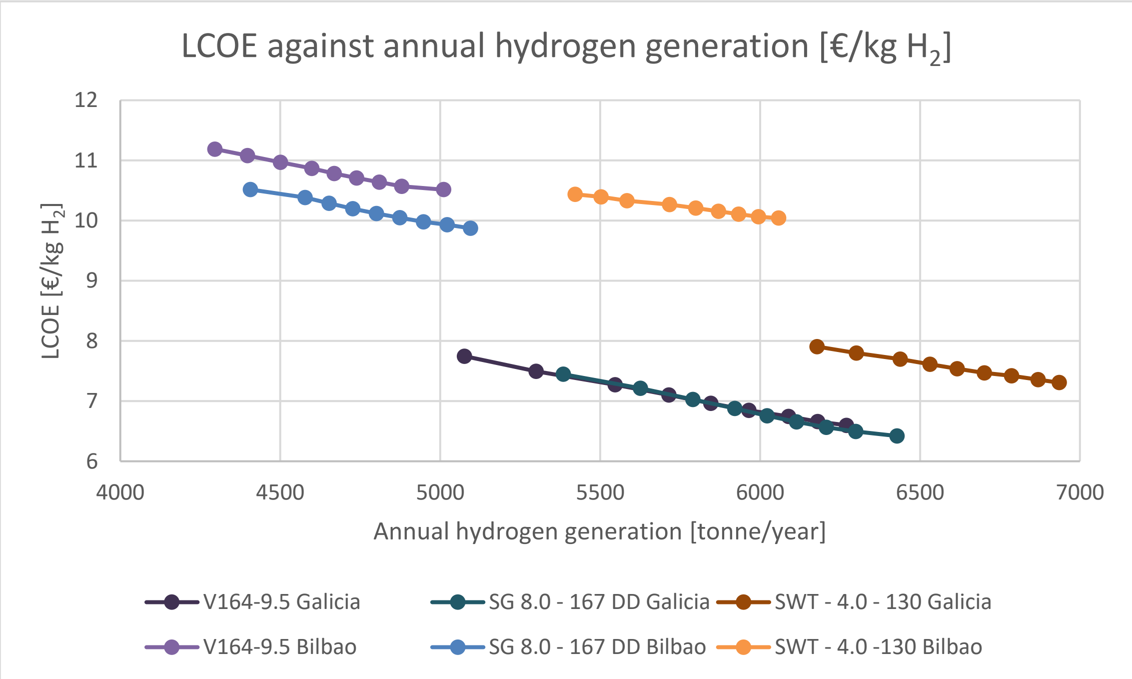

Figure 4-11: Hydrogen LCOE against hydrogen annual generation

As mentioned, if the wind farm is located in Galicia, the energy will have to be transported to Petronor, 500 km away. To carry out this transport, two solutions are proposed: to locate the electrolyser on the Galician coast and transport hydrogen by pipeline or to transport the electricity to Petronor and locate the electrolyser at that site. Table 4-16 shows the CAPEX of each solution, considering that the electricity transport can be carried out by HVAC or HVDC technologies, as well as the losses associated with each system.

Table 4-16: CAPEX and energy losses of energy transport from Galicia to the hydrogen consumption site

Solution	CAPEX [M€]	Energy losses [%]
Electricity: HVAC	265.85	19
Electricity: HVDC	249.66	5
Hydrogen	265.5	1

The use of HVAC transmission lines is excluded as the cost and losses are the highest. The hydrogen transport entails an extra cost due to the compression units needed along the pipeline, estimated at 0.6 €/kg.

Figure 4-12 shows the final hydrogen LCOE considering energy transport cost. It should be noted that the following assumptions have been made in these calculations:

- Electricity transport: electricity transport cost has been added to the wind farm CAPEX, thus, increasing the LCOE of the produced electricity.
- Hydrogen transport: transport costs have been added to the electrolyser CAPEX, assuming that the electricity LCOE remains unchanged.

For the same hydrogen production, electricity transmission is cheaper than using hydrogen pipes. For example, if is desired to obtain 6,000 tonnes of hydrogen per year, the most appropriate solution would be to use V164-9.5 turbines, achieving an LCOE of 10.08 €/kg H_2.

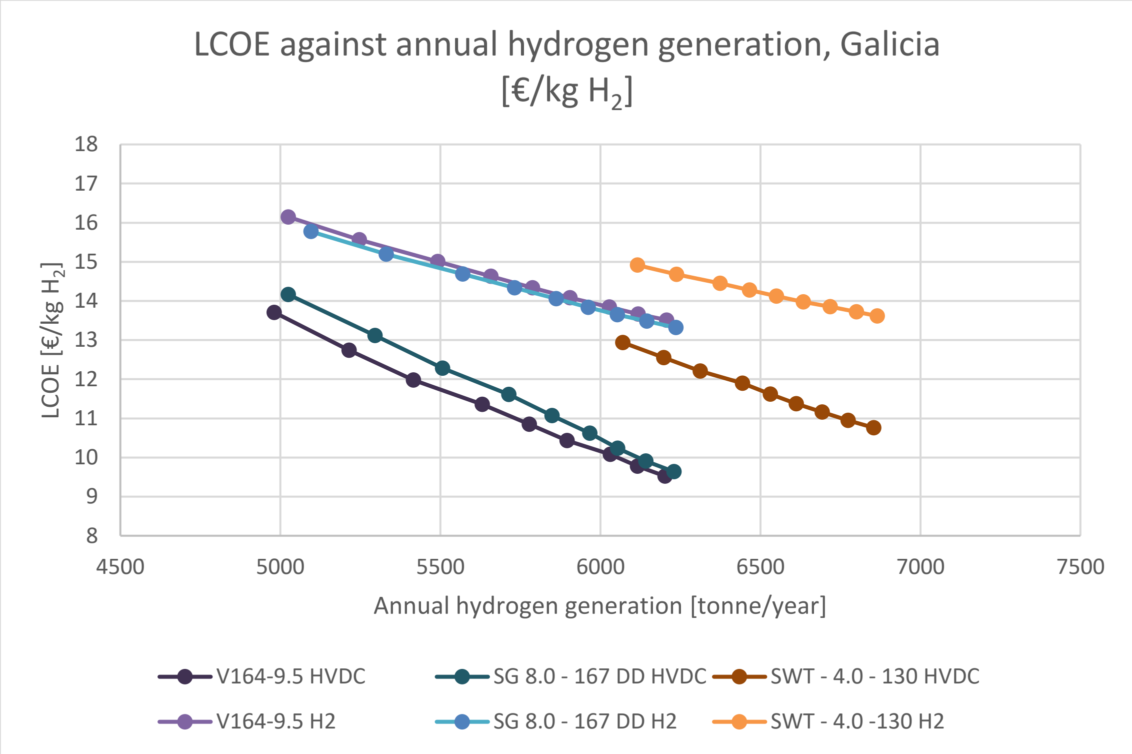

Figure 4-12: Hydrogen LCOE against hydrogen annual generation considering energy transport (Galicia)

The following figures show the final results obtained in terms of hydrogen production, annual electricity excess, and hydrogen and electricity LCOEs.

- Figure 4-13 shows a comparison of the hydrogen LCOE, assuming that electricity is produced in Galicia or Bilbao and that the electrolyser is located in Petronor.
- Figure 4-14 shows the electricity excess against hydrogen production.
- Figure 4-15 shows the electricity LCOE as a function of the electricity surplus.

To evaluate the results, a specific scenario has been considered, in which 6,000 tonnes of hydrogen are to be produced annually.

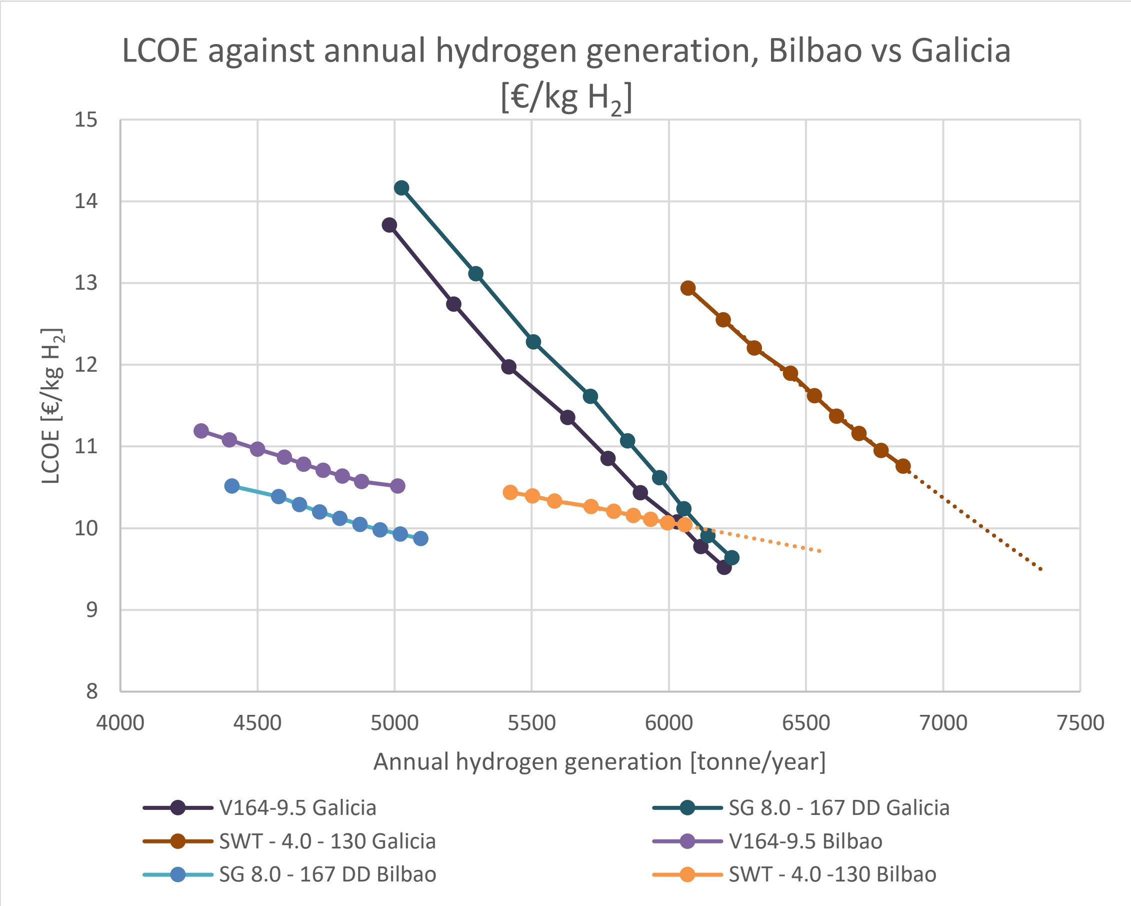

Figure 4-13: Hydrogen LCOE against hydrogen annual generation, Bilbao vs Galicia

In the range of 6,000 tonnes of hydrogen per year, three possible solutions are available:

- If the wind farm is located in Bilbao, the SWT-4.0-130 model should be used, achieving an LCOE of 10.04 €/kg H_2.
- However, if the wind farm is in Galicia, very similar results are obtained using V164-9.5 and SG 8.0-167 DD turbines, achieving LCOEs of 10.08 and 10.24 €/kg H_2, respectively.

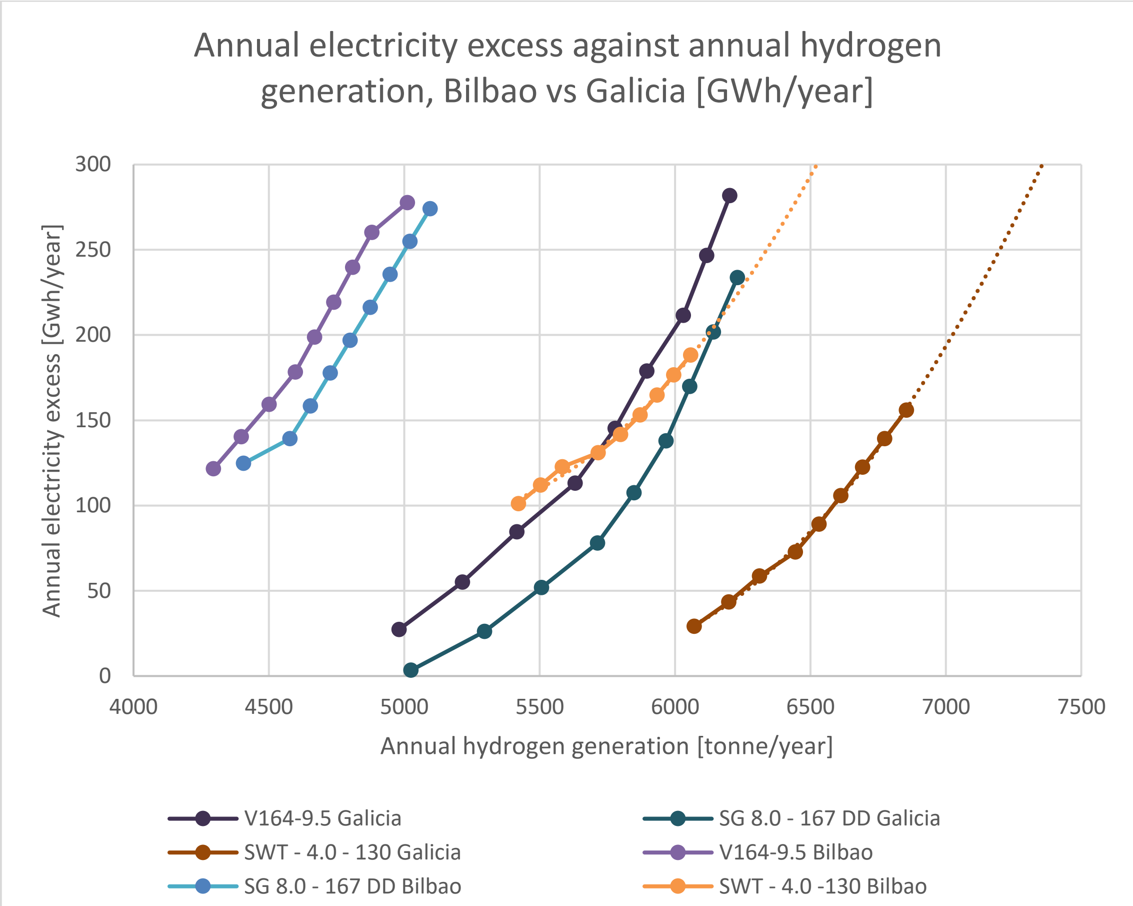

Figure 4-14: Annual electricity excess against hydrogen annual generation, Bilbao vs Galicia

Staying with the proposed example, if hydrogen production is 6,000 tonnes/year, the electricity excess will range between 169.84 GWh and 211.48 GWh, corresponding to an LCOE of 181.54 €/MWh and 178.44 €/MWh, respectively.

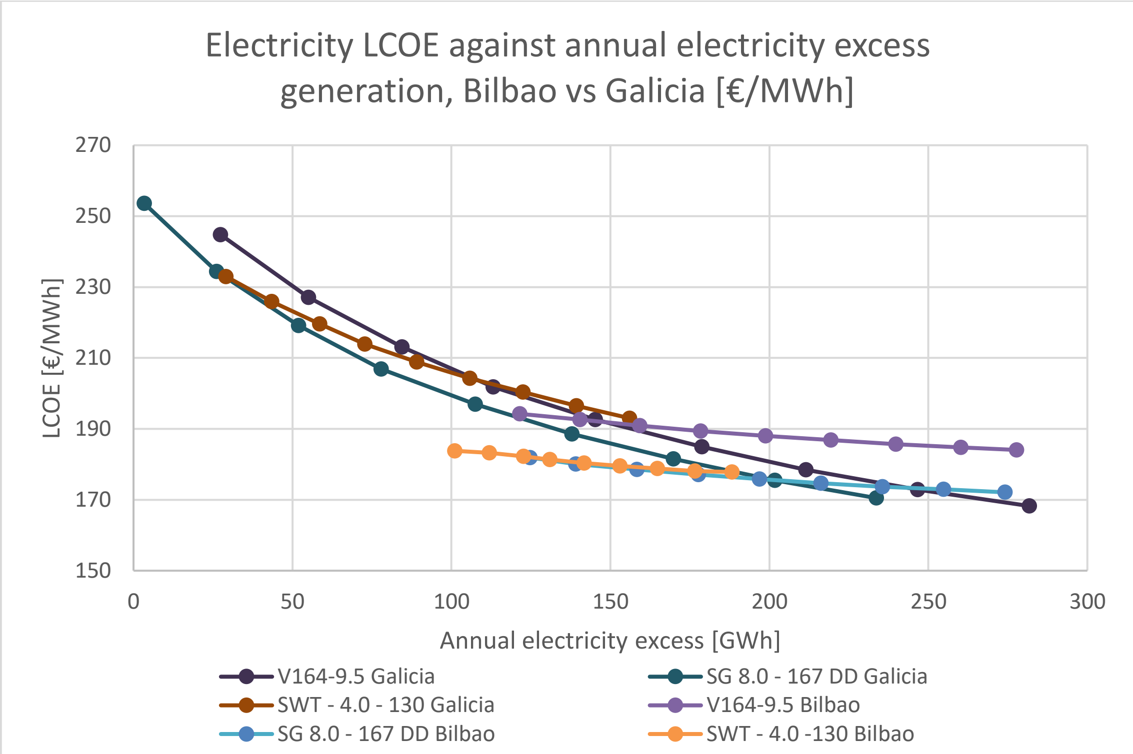

Figure 4-15: Electricity LCOE against annual electricity excess, Bilbao vs Galicia

Table 4-17 summarises the characteristics of the proposed solutions if the objective is the production of 6,000 tonnes of hydrogen per year:

Table 4-17: Solutions envisaged to produce 6,000 tonnes of hydrogen per year

	Solution		
Characteristics	1	2	3
Wind farm location	Bilbao	Galicia	Galicia
Turbine model	SWT-4.0-130	V164-9.5	SG8.0-167DD
Number of turbines	33	9	10
Annual H_2 production [tonne/year]	6,058.10	6,030.76	6,054.55
H_2 LCOE [€/kg H_2]	10.04	10.08	10.24
Annual electricity excess [GWh/year]	188.28	211.48	169.84
Electricity LCOE [€/MWh]	177.83	178.44	181.54

If the electricity excess management is a problem, a fourth solution could be considered using SWT-4.0-130 turbines in Galicia, as although the hydrogen LCOE is 12.94 €/kg H_2, the excess electricity is reduced to 29.12 GWh.

4.5 Sensitivity and cost analysis

The following section shows the results obtained from the cost analysis carried out using the @RISK software [64]. Firstly, of the individual subsystems (wind farm, electrolyser, and energy transport) and, then, of the overall system.

- **Wind farm:**

Scenarios G_0 and B_0 have been analysed for the three turbine models studied throughout the project: V164-9.5, SG 8.0-167 DD, and SWT-4.0-130. Figure 4-16, as an example, shows the result obtained for the B_0 scenario and V164-9.5 turbine model:

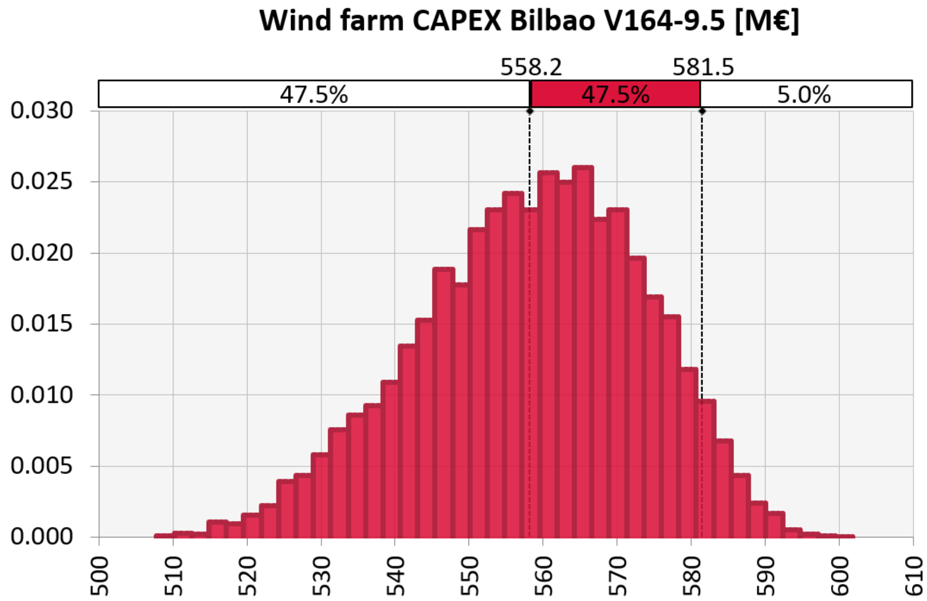

Figure 4-16: Probability of meeting the estimated budget for scenario G_0 and V164-9.5 turbine

Performing this analysis for each scenario provides the results shown in Table 4-18:

Table 4-18: Probability of staying within the wind farm budget

	Probability of meeting the budget		
Scenario	V164-9.5	SG 8.0-167 DD	SWT-4.0-130
G_0	38.8%	37.2%	30.3%
B_0	47.5%	45.3%	37.8%

The probability that the CAPEX remains equal to or lower than the calculated value ranges between 30.3% and 47.5%, this percentage is higher when the turbines' rated power is higher, probably because fewer turbines are needed to generate the same annual electricity. However, it should be noted that it is more likely to stay within the budget when the wind farm is located in Bilbao than in Galicia.

The contribution to the variance of each variable has been obtained to determine which variables dominate the results. Figure 4-17 shows the results obtained for the example shown above (Figure 4-16):

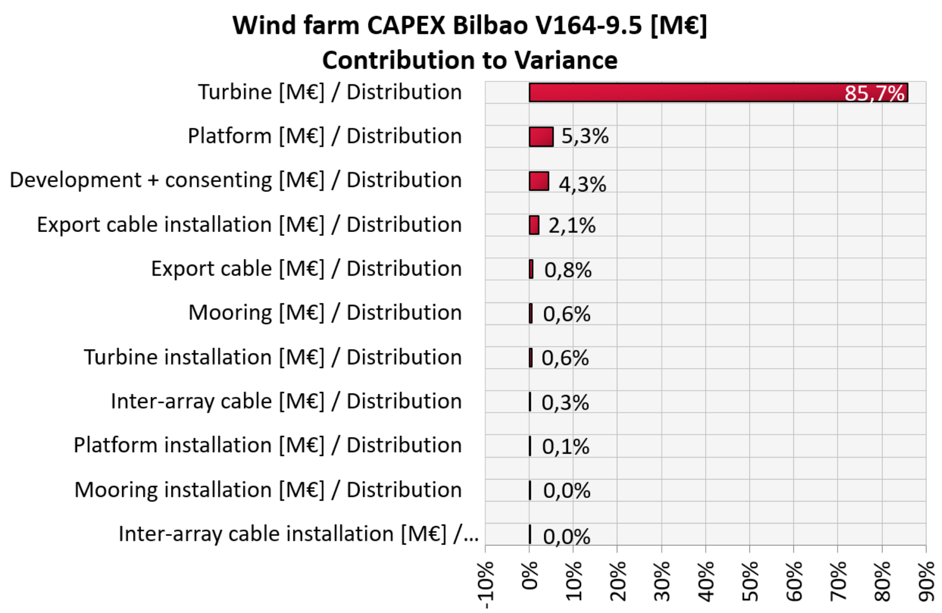

Figure 4-17: Contribution to variance for scenario G_0 and V164-9.5 turbine

The most influential variable is the turbine cost, because although the unit cost does not vary significantly (+8%, -20%), the nominal capacity of the wind farm is high, which makes the total turbines cost high. In the second place, with 5.3%, is the cost of the offshore platform, which remains constant for all scenarios, but has high variability, around +29% and -20%. Development and consenting costs also depend on the wind farm capacity and have a variability of +20% and -27%.

Table 4-19 and Table 4-20 show the contribution to the variance of the budget items:

Table 4-19: Contribution to variance, wind farms located in Galicia

	Contribution to Variance (G_0)			
Turbine model	Turbine	Offshore platform	Development and consenting	Export cable installation
V164-9.5	73%	10%	3.7%	3.7%
SG 8.0-167 DD	83.4%	6.6%	4.3%	2.6%
SWT-4.0-130	85.4%	5.8%	4.2%	2.1%

Table 4-20: Contribution to variance, wind farms located in Bilbao

	Contribution to Variance (B_0)				
Turbine model	Turbine	Offshore platform	Export cable installation	Export cable	Development and consenting
V164-9.5	59%	16%	11%	4.4%	2.9%
SG 8.0-167 DD	68.2%	13.4%	9.4%	3.6%	3.4%
SWT-4.0-130	71.1%	12.3%	8.2%	3.2%	3.6%

In all cases, the dominant variable is the turbine cost; however, this value is reduced as the power of the wind farm decreases and is lower in Galicia than in Bilbao. This may be since by reducing the turbine number, the proportion of the budget allocated to this item is lower, reducing its variability. Secondly, the offshore platform cost, which remains constant in all scenarios, has a greater impact when the total cost of the wind farm is lower.

The next most influential parameters vary from one location to another. Development and consenting costs depend on the wind farm capacity, as does the turbine cost, following the same trend. On the other hand, both the export cable cost and its installation depend on the cable length, being constant for each location and gaining importance when the wind farm total cost is lower.

- **Electrolyser:**

Figure 4-18 shows the probability of meeting the calculated hydrogen LCOE when the electrolyser is operated at the maximum capacity factor (92%) and the grid electricity price is considered. It can be seen that the probability of staying within the budget is higher if the alkaline electrolyser is used and, in addition, the maximum LCOE is lower.

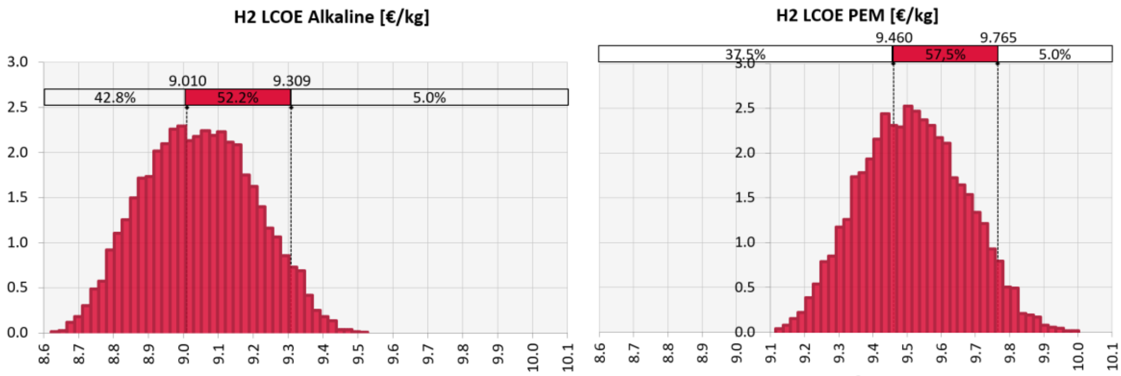

Figure 4-18: Probability of meeting the hydrogen LCOE: alkaline vs PEM

Electrolyser efficiency is the variable that most significantly affects the variance (91.9% and 83.2% for the alkaline and PEM electrolyser), followed by CAPEX and finally OPEX (2.1% and 0.8%, respectively).

- **Energy transport:**

Figure 4-19 shows the results obtained for the electricity transport cost when the type of cable used is HVDC or HVAC. If the HVDC technology is used, the cost is bounded in a narrower range, achieving a 51.7% probability of staying within the budget, compared to 50% for HVAC.

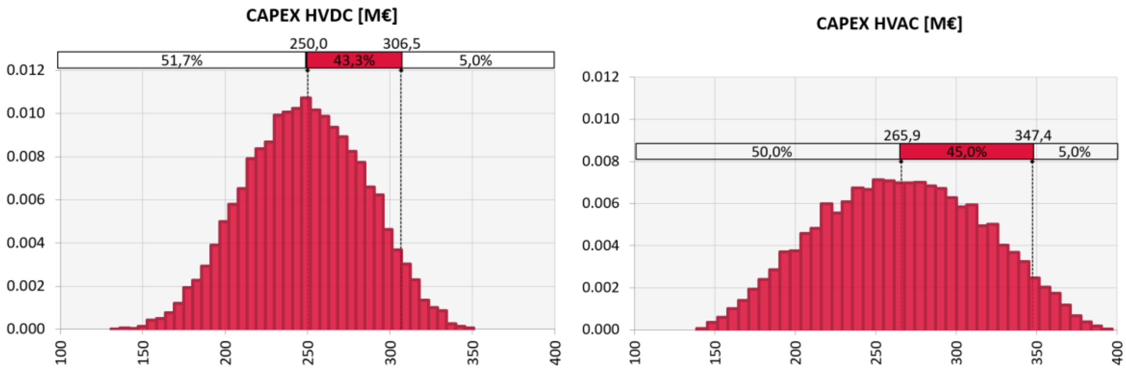

Figure 4-19: Probability of achieving estimated CAPEX for HVDC and HVAC technologies

The CAPEX variance is dominated by the cable cost, achieving 76.8% for HVDC transmission lines and 99.9% for HVAC, which shows that the substation cost hardly affects the result. Based on this analysis, the HVDC system is more appropriate for this project.

As for hydrogen transport, the probability of staying within the budget is 44% and the 95% expected budget is 432.7 M€, higher than any of the electricity transmission options.

- **Total:**

Once the analysis by subsystems has been carried out, how each subsystem affects the total cost has been analysed. As an example, Figure 4-20 and Figure 4-21 show the results obtained when using V164-9.5 turbines in Galicia and Bilbao.

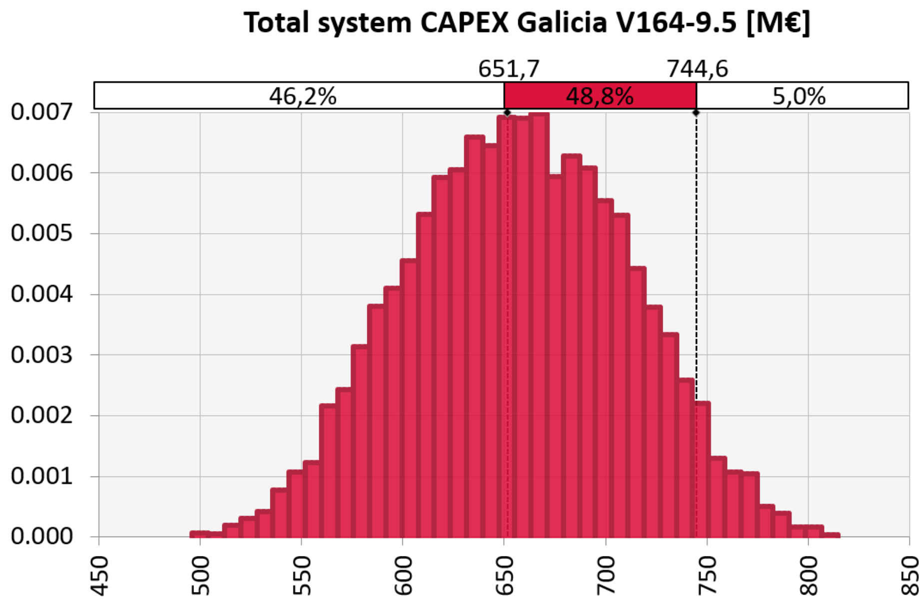

Figure 4-20: Probability of meeting total CAPEX (Galicia, turbine model V164-9.5)

If the wind farm is located in Galicia and the electrolyser in Bilbao, with the electricity being transmitted from one location to the other via an HVDC line, the total CAPEX of the system varies greatly, ranging from 463.04 to 870.23 M€.

Electricity transport is the variable that contributes most to the variance (80.5%), followed by the wind farm (18.9%) and, lastly, the electrolyser (0.6%).

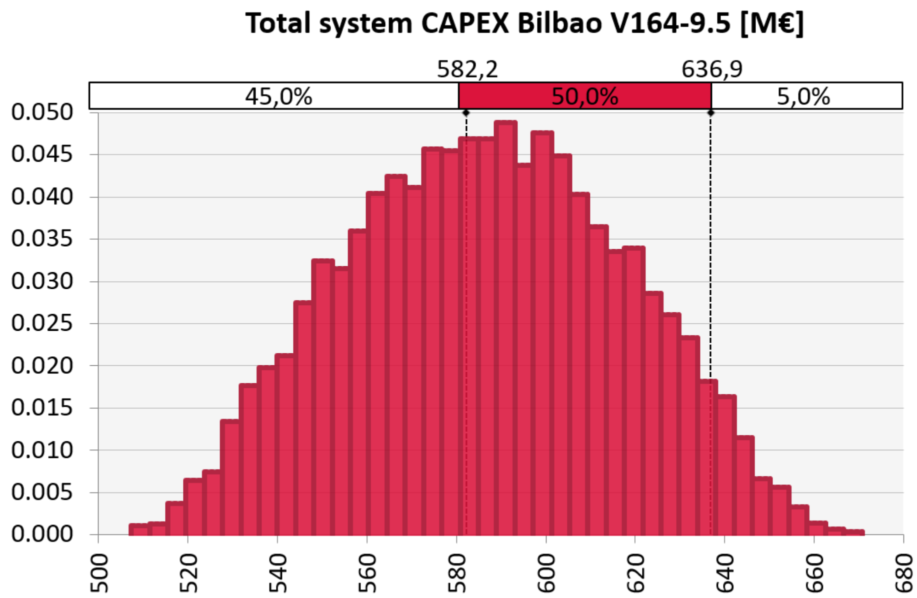

Figure 4-21: Probability of meeting total CAPEX (Bilbao, turbine model V164-9.5)

If the wind farm is located in Bilbao, the total CAPEX ranges between 500.5 and 689.3 M€, which is a narrower range than in the previous scenario. This is because the HVDC transmission line, which is a major source of uncertainty, is not required. In this case, the contribution to the variance is dominated by the wind farm, reaching 98.2%. Figure 4-22 shows how different the two probability distributions are:

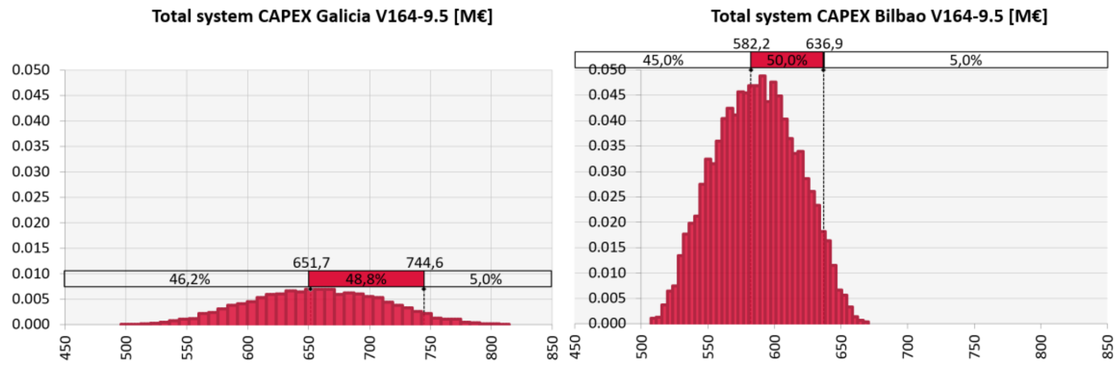

Figure 4-22: Comparison of the probability distributions, Galicia vs Bilbao

4.5.1 Comparison of minimum and maximum scenarios

Once the variability of the systems' cost has been analysed, the best and worst results that could be achieved in each scenario have been studied. In other words, what would be the lowest and the highest LCOE that could be obtained according to the assumptions indicated in Section 3.10.2.

Table 4-21 and Table 4-22 show the electricity LCOE at the generation place, i.e. without considering the electricity transport to the consumption location.

Table 4-21: Electricity LCOE at the electricity generation location (Galicia)

	Electricity LCOE Galicia [€/MWh]		
Probability	V164-9.5	SG 8.0-167 DD	SWT-4.0-130
5%	114.62	111.64	128.41
G_0	118.71	115.21	131.28
95%	123.72	120.11	136.5

Table 4-22: Electricity LCOE at the electricity generation location (Bilbao)

	Electricity LCOE Bilbao [€/MWh]		
Probability	V164-9.5	SG 8.0-167 DD	SWT-4.0-130
5%	151.73	169.39	175.69
B_0	188.01	175.83	180.35
95%	194.65	181.91	186.27

As can be seen, in any case, the electricity LCOE, excluding transport cost, is lower if the wind farm is located in Galicia, as the maximum LCOE that can be obtained in this location (136.5 €/MWh) is lower than the minimum that could be obtained in Bilbao (151.73 €/MWh).

As for the hydrogen LCOE, Table 4-23 shows the results obtained when the wind farm is located in Galicia and energy is transported to Petronor by HVDC lines or H_2 pipelines:

Table 4-23: Hydrogen LCOE if the wind farm is located in Galicia

	H_2 LCOE HVDC line [€/kg H_2]			H_2 LCOE H_2 pipeline [€/kg H_2]		
Probability	V164-9.5	SG 8.0-167 DD	SWT-4.0-130	V164-9.5	SG 8.0-167 DD	SWT-4.0-130
5%	9.76	10.30	10.55	11.21	10.99	11.4
G_0	10.85	11.06	11.62	14.33	14.06	14.12
95%	11.93	12.63	12.75	18.86	18.32	18.16

From this comparison, it can be deduced that, although a lower LCOE could be obtained using pipelines, the probability of reaching this result is only 5%, so its use in this project is ruled out.

Table 4-24 shows the hydrogen LCOE when the wind farm is located in Bilbao:

Table 4-24: Hydrogen LCOE if the wind farm is located in Bilbao

	H_2 LCOE Bilbao [€/kg H_2]		
Probability	V164-9.5	SG 8.0-167 DD	SWT-4.0-130
5%	8.88	9.78	9.96
B_0	10.78	10.12	10.21
95%	11.13	10.44	10.52

For the same probability of achievement, lower LCOEs are obtained if the wind farm is located in Bilbao and it can therefore be concluded that this should be the wind farm location.

It is also interesting to analyse what the optimum solution would be if the hydrogen demand were to be transferred to Galicia. In this new context, the infrastructure needed to transport energy from Galicia to Bilbao would not be required and the results shown in Table 4-25 would be obtained:

Table 4-25: Hydrogen LCOE if the wind farm and hydrogen demand are in Galicia

	H_2 LCOE Galicia [€/kg H_2]		
Probability	V164-9.5	SG 8.0-167 DD	SWT-4.0-130
5%	6.75	6.57	7.39
G_0	6.96	6.76	7.54
95%	7.23	7.01	7.81

Results obtained for this new context are more competitive, as regardless of the turbine model used and with a 95% probability of staying within the budget, the hydrogen LCOE is lower than the results shown in Table 4-24, corresponding to placing the wind farm in Bilbao.

5 CONCLUSIONS AND RECOMMENDATIONS

Establishing hydrogen production infrastructure from renewable energy is a high priority for the energy transition, for which both the possible demands and location of electrolysis and energy generation must be analysed. The development of green hydrogen production will be driven mainly by industries that currently use hydrogen, especially oil refineries such as Petronor, located on the Cantabrian Coast (Spain). As for the source of renewable generation, although there is currently no offshore wind installed in Spain, due to the narrow Spanish continental shelf, the development of new floating systems will make it possible to develop this technology in sites up to 1,000 m deep.

Within this context, the coupling of both systems and their possible development in the Spanish North-Atlantic area is studied in this project, in addition to analysing the resilience of the results obtained and the main variables that dominate design decision-making. This last is especially important because floating offshore wind technology is still under development, no commercial-scale plant has been deployed in Spain, and, therefore, neither has the coupling of both technologies. Consequently, the study of the uncertainty of the project cost is critical in the analysis of the feasibility of the project.

@RISK software has been used to carry out the sensitivity analysis, which through Monte Carlo simulations, provides the probability of staying within the calculated budget, defining its reliability. The variables that contribute most significantly to the system cost variance have also been analysed. To do so, the wind farm, the electrolyser, and the energy transport have been studied separately.

Firstly, the wind resource potential and the wind farm design have been studied, analysing turbines of different rated power. In addition to being greater, the wind resource on the Atlantic Coast is more uniform than on the Cantabrian Coast, allowing higher capacity factors to be achieved. The highest capacity factors are obtained with small turbines (around 65% on the Atlantic Coast), while high-rated power turbines offer a higher annual electricity production, almost double.

The number of wind turbines that make up the farm has been estimated on the assumption that it should cover the annual energy demand of a 50 MW electrolyser (424.17 GWh/year). Thus, fewer turbines are needed when high-quality wind resources and high-power wind turbines are available, which results in a decrease in the electricity LCOE (from 27.2% to 36.9% for SWT-4.0-130 and V164-9.5 turbine models, respectively). For a certain location and turbine model, increasing the wind farm turbine number reduces the electricity LCOE due to the effect of fixed costs. Taking the Atlantic Coast and the SG 8.0-167 DD turbine model as an example, increasing 8 the number of turbines, reduces the electricity LCOE by 13.5%. In addition, the economies of scale reduce the project costs, although their impact has not been considered in this project.

The probability of staying within the calculated wind farm CAPEX ranges from 30.3% to 47.5%, obtaining higher results when the rated power of the turbines is higher. In fact, it is the cost of the turbines that contributes most to the deviation (between 59.0% and 85.4%), as although the unit cost variation is low, the power capacity of the wind farm is high, making the total cost of the turbines the most important item in the CAPEX. The next most significant variable is the offshore platform cost, which has been considered constant, and therefore becomes more important when the total cost of the wind farm is lower.

With regard to the type of electrolyser to be used, proton exchange membrane (PEM) and alkaline electrolysers have been studied in this project. With the technology available today, the alkaline electrolyser offers better performance, obtaining higher hydrogen production at a lower cost, despite having a lower operating range. In addition, the probability of staying within the calculated LCOE is higher (42.8% and 37.5% for alkaline and PEM electrolysers, respectively).

However, it is worth mentioning that it has been assumed that the only power source for the electrolyser is the wind farm and that no energy storage is used.

This implies that the capacity factor of the electrolyser decreases and that it will only operate at full load for around 38.8-56.3% of the year. Working at partial load deteriorates the performance of the electrolyser, especially in alkaline electrolysers. This effect has not been considered in the project but it would be interesting to analyse it in future studies since depending on the degree of degradation, it could be more interesting to use a PEM electrolyser, which works better at partial load, or to consider a combined power supply: using the wind farm electricity when possible and when not, supplying the electrolyser with grid electricity, even if this would mean that the hydrogen produced would not be fully renewable, as electricity from the Spanish grid is not renewable at the moment.

As mentioned, installing the wind farm on the Atlantic Coast offers several advantages, however, it is located about 500 km from the hydrogen consumption location. Two possible alternatives have been studied: transporting the electricity to Petronor, where an electrolyser would produce hydrogen, or producing it in Galicia and transporting it via pipelines. For electricity transmission, HVDC lines are the most suitable technology, offering advantages such as simplicity of construction or fewer corona losses than HVAC. However, substations are costlier and more complex. Compared to this technology, hydrogen pipelines have a higher cost and greater variability, which increases the risk and uncertainty of the technology. The construction of energy transmission systems, for both electricity and hydrogen, involves extra risks associated with environmental constraints, including social implications.

Within this context, being Petronor the hydrogen demand location, several options are considered when determining the optimal solution: both in terms of location and system characteristics. If the wind farm is located on the Cantabrian Coast, energy transport is not required, which significantly reduces the variability of the project CAPEX and, therefore, its resilience. Indeed, if the wind farm is located on the Cantabrian Coast, the variability of the project CAPEX is around +/-15%, while if it is located on the Atlantic Coast, it is +/-30%.

However, to produce the same annual electricity on the Cantabrian Coast as on the Atlantic Coast, a greater number of turbines is required (around 50%), the nominal capacity of the wind farm being much higher than that of the electrolyser. This means that of the annual electricity production, the fraction destined for hydrogen production is lower, increasing the surplus electricity that has to be managed (it could be sold to the grid or used for other purposes in the refinery). Thus, the number of turbines to be installed depends on the hydrogen demand and the capacity to manage the surplus electricity.

On the other hand, it is interesting to analyse what would happen if the context of the project would change, and instead of requiring the hydrogen in Petronor (Bilbao), the demand would be transferred to the region of Galicia. The LCOE of the electricity produced by a wind farm located on the Atlantic Coast is lower than that obtained on the Cantabrian Coast and the production is also more uniform. These characteristics would make Galicia an attractive location for the development of the coupling of offshore wind and hydrogen production by electrolysis, as competitive LCOEs of about 115.21 €/MWh for electricity and 6.76 €/kg for hydrogen could be achieved.

From developing the initial methodology of the project, aimed at proposing the optimum design for powering a 50 MW electrolyser using offshore wind energy, being Petronor the final destination of hydrogen consumption, the research then examines the sensitivity of the results obtaining a decision-making tool for designing a system of these characteristics in northern Spain. In each case, this decision tool allows consideration of the possible options for the location and design of the wind farm, as well as the electrolyser, determining the annual hydrogen and electricity production. It also enables the definition of the products' LCOE, as well as their probability of achievement, which is of particular importance as it indicates the project's viability.

REFERENCES

[1] Ministry for Ecological Transition and the Demographic Challenge, ‘Hoja de ruta del hidrógeno: Una apuesta por el hidrógeno renovable’, Madrid, Oct. 2020.

[2] Petronor, ‘Petronor página oficial’, 2022. https://petronor.eus/es/ (accessed Jun. 24, 2022).

[3] Repsol, ‘Plan de Sostenibilidad 2021 Petronor’, 2021.

[4] Petronor, ‘Petronor instala un electrolizador de 2,5 MW como primer paso del Corredor Vasco del Hidrógeno’, Sep. 20, 2021. https://petronor.eus/es/2021/09/petronor-instala-un-electrolizador-de-25-mw-como-primer-paso-del-corredor-vasco-del-hidrogeno/ (accessed Jun. 24, 2022).

[5] BH2C, ‘Basque Hydrogen Corridor’, 2022. https://www.bh2c.org/en (accessed Jun. 21, 2022).

[6] C. Fetting, ‘The European Green Deal’, Vienna, Dec. 2020.

[7] United Nations, ‘Paris Agreement’, Paris, Dec. 2015.

[8] MITECO, ‘Estrategia de descarbonización a largo plazo 2050’, Madrid, Nov. 2020.

[9] Spanish Government, ‘Integrated National Energy and Climate Plan 2021-2030’, Jan. 2020. Accessed: Jun. 20, 2022. [Online]. Available: https://ec.europa.eu/energy/sites/ener/files/documents/es_final_necp_main_en.pdf

[10] European Commission, ‘A hydrogen strategy for a climate-neutral Europe’, Brussels, Jul. 2020. Accessed: Jun. 21, 2022. [Online]. Available: https://www.eu2018.at/calendar-events/political-events/BMNT-

[11] Ministry for Ecological Transition and the Demographic Challenge, ‘Roadmap Offshore Wind and Marine Energy in Spain’, Madrid, Mar. 2022.

[12] European Commission, ‘Offshore Renewable Energy Strategy’, Nov. 2020. doi: 10.2833/756349.

[13] IRENA, *Offshore renewables: An action agenda for deployment*. Abu Dhabi: International Renewable Energy Agency, 2021. [Online]. Available: www.irena.org

[14] N. Bento and M. Fontes, ‘Emergence of floating offshore wind energy: Technology and industry’, *Renewable and Sustainable Energy Reviews*, vol. 99, pp. 66–82, Jan. 2019, doi: 10.1016/J.RSER.2018.09.035.

[15] J. Aymami, A. García, O. Lacave, L. Lledo, M. Mayo, and S. Parés, ‘Análisis del recurso. Atlas eólico de España (Estudio técnico PER 2011-2020)’, Madrid, 2011. Accessed: Jun. 24, 2022. [Online]. Available: https://www.idae.es/uploads/documentos/documentos_11227_e4_atlas_eolico_A_9b90ff10.pdf

[16] Energy Sector Management Assistance Program, ‘Offshore Wind Technical Potential - Analysis and Maps | ESMAP’, 2022. https://esmap.org/esmap_offshorewind_techpotential_analysis_maps (accessed Jun. 24, 2022).

[17] ‘Global Wind Atlas’. https://globalwindatlas.info/ (accessed Jun. 24, 2022).

[18] IEA, ‘Offshore Wind Outlook 2019’, Paris, 2019. Accessed: Jun. 21, 2022. [Online]. Available: www.iea.org/t&c/

[19] E. Lozano-Minguez, A. J. Kolios, and F. P. Brennan, ‘Multi-criteria assessment of offshore wind turbine support structures’, *Renew Energy*, vol. 36, no. 11, pp. 2831–2837, Nov. 2011, doi: 10.1016/J.RENENE.2011.04.020.

[20] L. Castro-Santos, A. R. Bento, D. Silva, N. Salvação, and C. Guedes Soares, 'Marine Science and Engineering Economic Feasibility of Floating Offshore Wind Farms in the North of Spain', *Marine Science and Engineering*, Jan. 2020, doi: 10.3390/jmse8010058.

[21] A. Martinez and G. Iglesias, 'Mapping of the levelised cost of energy for floating offshore wind in the European Atlantic', *Renewable and Sustainable Energy Reviews*, vol. 154, Feb. 2022, doi: 10.1016/J.RSER.2021.111889.

[22] S. Butterfield, W. Musial, J. Jonkman, and P. Sclavounos, 'Engineering Challenges for Floating Offshore Wind Turbines', 2005, Accessed: Jun. 11, 2022. [Online]. Available: http://www.osti.gov/bridge

[23] W. Wisatesajja, W. Roynarin, and D. Intholo, 'Comparing the Effect of Rotor Tilt Angle on Performance of Floating Offshore and Fixed Tower Wind Turbines', *J Sustain Dev*, vol. 12, no. 5, p. 84, Sep. 2019, doi: 10.5539/jsd.v12n5p84.

[24] H. Díaz, S. Loughney, J. Wang, and C. Guedes Soares, 'Comparison of multicriteria analysis techniques for decision making on floating offshore wind farms site selection', *Ocean Engineering*, vol. 248, Mar. 2022, doi: 10.1016/j.oceaneng.2022.110751.

[25] L. Castro-Santos, M. I. Lamas-Galdo, and A. Filgueira-Vizoso, 'Managing the oceans: Site selection of a floating offshore wind farm based on GIS spatial analysis', *Mar Policy*, vol. 113, Mar. 2020, doi: 10.1016/j.marpol.2019.103803.

[26] R. d'Amore-Domenech, Ó. Santiago, and T. J. Leo, 'Multicriteria analysis of seawater electrolysis technologies for green hydrogen production at sea', *Renewable and Sustainable Energy Reviews*, vol. 133, Nov. 2020, doi: 10.1016/j.rser.2020.110166.

[27] M. A. Khan *et al.*, ‘Seawater electrolysis for hydrogen production: A solution looking for a problem?’, *Energy Environ Sci*, vol. 14, no. 9, pp. 4831–4839, Sep. 2021, doi: 10.1039/D1EE00870F.

[28] A. Mohammadi and M. Mehrpooya, ‘A comprehensive review on coupling different types of electrolyzer to renewable energy sources’, *Energy*, vol. 158, pp. 632–655, Sep. 2018, doi: 10.1016/j.energy.2018.06.073.

[29] M. Niermann, S. Timmerberg, S. Drünert, and M. Kaltschmitt, ‘Liquid Organic Hydrogen Carriers and alternatives for international transport of renewable hydrogen’, *Renewable and Sustainable Energy Reviews*, vol. 135, Jan. 2021, doi: 10.1016/J.RSER.2020.110171.

[30] A. M. Abdalla, S. Hossain, O. B. Nisfindy, A. T. Azad, M. Dawood, and A. K. Azad, ‘Hydrogen production, storage, transportation and key challenges with applications: A review’, *Energy Convers Manag*, vol. 165, pp. 602–627, Jun. 2018, doi: 10.1016/J.ENCONMAN.2018.03.088.

[31] BloombergNEF, ‘Hydrogen Economy Outlook’, Mar. 2020.

[32] A. Rödl, C. Wulf, and M. Kaltschmitt, ‘Assessment of Selected Hydrogen Supply Chains—Factors Determining the Overall GHG Emissions’, *Hydrogen Supply Chain: Design, Deployment and Operation*, pp. 81–109, Jan. 2018, doi: 10.1016/B978-0-12-811197-0.00003-8.

[33] TCI GECOMP and H2Chile, ‘ESTUDIO DE INSTALACIÓN DE GENERACION DE HIDRÓGENO 100 MW’.

[34] IEA, ‘The Future of Hydrogen’, Jun. 2019.

[35] P. Boira, ‘El precio baja en la subasta de energía tras la aplicación de la excepción ibérica en el mercado mayorista’, *Newtral*, Jun. 14, 2022. https://www.newtral.es/precio-luzbaja-tope-excepcion-iberica/20220614/ (accessed Jul. 31, 2022).

[36] Google Maps, ‘Google Maps’. https://www.google.com/maps/ (accessed Aug. 04, 2022).

[37] Gobierno de España, ‘Prediccion de oleaje, nivel del mar ; Boyas y mareografos’, *Puertos del Estado*. https://www.puertos.es/es-es/oceanografia/Paginas/portus.aspx (accessed Jul. 31, 2022).

[38] F. Bañuelos-Ruedas, C. Ángeles Camacho, and S. Rios-Marcuello, ‘Methodologies Used in the Extrapolation of Wind Speed Data at Different Heights and Its Impact in the Wind Energy Resource Assessment in a Region’, 2011, Accessed: Jul. 31, 2022. [Online]. Available: www.intechopen.com

[39] J. Guzmán Chaves, ‘Estudio técnico preliminar y viabilidad económica de parque eólico offshore en Faro Punta Nariga (Galicia) mediante el vehículo inversor de project finance’, Universidad de Cantabria, Santander, 2021.

[40] Vestas, ‘V164-9.5 MW™’. https://www.vestas.com/en/products/offshore/V164-9-5-MW (accessed Jul. 31, 2022).

[41] Siemens-Gamesa, ‘SG 8.0-167 DD ’, Zamudio, Vizcaya, Spain.

[42] Siemens-Gamesa, ‘SWT-6.0-154 ’. https://www.siemensgamesa.com/products-and-services/offshore/wind-turbine-swt-6-0-154 (accessed Jul. 31, 2022).

[43] Siemens-Gamesa, ‘SWT-DD-130’. https://www.siemensgamesa.com/-/media/siemensgamesa/downloads/en/products-and-services/onshore/data-sheets/siemens-gamesa-onshore-wind-turbine-swt-dd-130-en.pdf (accessed Jul. 31, 2022).

[44] The Wind Power, ‘SWT-4.0-130’, Jun. 04, 2018. https://www.thewindpower.net/turbine_en_957_siemens_swt-4.0-130.php (accessed Jul. 31, 2022).

[45] The Wind Power, ‘SWT-6.0-154’, Jun. 04, 2018. https://www.thewindpower.net/turbine_es_807_siemens_swt-6.0-154.php (accessed Jul. 31, 2022).

[46] The Wind Power, 'SG 8.0-167 DD', May 11, 2022. https://www.thewindpower.net/turbine_es_1558_siemens-gamesa_sg-8.0-167-dd.php (accessed Jul. 31, 2022).

[47] The Wind Power, 'Vestas V164/9500', Jul. 08, 2022. https://www.thewindpower.net/turbine_en_1476_mhi-vestas-offshore_v164-9500.php (accessed Jul. 31, 2022).

[48] S. El-Asha, L. Zhan, and G. V. Iungo, 'Quantification of power losses due to wind turbine wake interactions through SCADA, meteorological and wind LiDAR data', *Wind Energy*, vol. 20, no. 11, pp. 1823–1839, Nov. 2017, doi: 10.1002/WE.2123.

[49] M. Nandigam and S. K. Dhali, 'Optimal Design of an Offshore Wind Farm Layout', *International Symposium on Power Electronics, Electrical Drivers, Automation and Motion*, pp. 1470–1474, 2008, Accessed: Jul. 13, 2022. [Online]. Available: https://ieeexplore.ieee.org/stamp/stamp.jsp?tp=&arnumber=4581308&isnumber=4581062

[50] Principle Power Inc., 'The WindFloat®', 2022. https://www.principlepower.com/windfloat (accessed Aug. 01, 2022).

[51] C. Bjerkseter and A. Agotnes, 'Levelised costs of energy for offshore floating wind turbine concepts', Norwegian University of Life Sciences, As, 2013.

[52] A. Myhr, C. Bjerkseter, A. Ågotnes, and T. A. Nygaard, 'Levelised cost of energy for offshore floating wind turbines in a lifecycle perspective', *Renew Energy*, vol. 66, pp. 714–728, 2014, doi: 10.1016/j.renene.2014.01.017.

[53] R. L. Jaffe and W. Taylor, *The Physics of Energy* . Cambridge University Press, 2018. Accessed: Aug. 02, 2022. [Online]. Available: https://books.google.es/books?id=drZDDwAAQBAJ&pg=PA552&lpg=PA552&dq=distance+between+turbines+direction+perpendicular+to+the+wind

&source=bl&ots=uYUVAL8N9i&sig=ACfU3U20CjFLPn0JJ48R1StPZT1rs40V9w&hl=es&sa=X&ved=2ahUKEwjn-uPN0qf5AhWlzIUKHU_dApUQ6AF6BAg5EAM#v=onepage&q=distance%20between%20turbines%20direction%20perpendicular%20to%20the%20wind&f=false

[54] M. F. Howland, S. K. Lele, and J. O. Dabiri, ‘Wind farm power optimization through wake steering’, *Proc Natl Acad Sci U S A*, vol. 116, no. 29, pp. 14495–14500, 2019, doi: 10.1073/PNAS.1903680116/-/DCSUPPLEMENTAL.

[55] B. Johnston, A. Foley, J. Doran, and T. Littler, ‘Levelised cost of energy, A challenge for offshore wind’, *Renew Energy*, vol. 160, pp. 876–885, Nov. 2020, doi: 10.1016/J.RENENE.2020.06.030.

[56] CFI Team, ‘Levelized Cost of Energy (LCOE)’, Jun. 21, 2022. https://corporatefinanceinstitute.com/resources/knowledge/finance/levelized-cost-of-energy-lcoe/ (accessed Aug. 02, 2022).

[57] K. Meier, ‘Hydrogen production with sea water electrolysis using Norwegian offshore wind energy potentials: Techno-economic assessment for an offshore-based hydrogen production approach with state-of-the-art technology’, *International Journal of Energy and Environmental Engineering*, vol. 5, no. 2–3, pp. 1–12, Jul. 2014, doi: 10.1007/s40095-014-0104-6.

[58] A. Singlitico, J. Østergaard, and S. Chatzivasileiadis, ‘Onshore, offshore or in-turbine electrolysis? Techno-economic overview of alternative integration designs for green hydrogen production into Offshore Wind Power Hubs’, *Renewable and Sustainable Energy Transition*, vol. 1, p. 100005, Aug. 2021, doi: 10.1016/J.RSET.2021.100005.

[59] 4e, giz, and frv, ‘Posibles modelos de negocio para proyectos de hidrógeno verde: Offtakers y aplicaciones del hidrógeno y sus derivados, costos asociados, logística y periodos de construcción, O&M y análisis de casos de éxito de proyectos de hidrógeno verde’, Aug. 2021.

[60] K. Meah and S. Ula, ‘Comparative Evaluation of HVDC and HVAC Transmission Systems’, *IEEE Power Engineering Society General Meeting*, pp. 1–5, 2007, Accessed: Aug. 04, 2022. [Online]. Available: https://ieeexplore.ieee.org/stamp/stamp.jsp?tp=&arnumber=4275759

[61] F. H. Saadi, N. S. Lewis, and E. W. Mcfarland, ‘Relative costs of transporting electrical and chemical energy’, *Energy Environ. Sci*, vol. 11, p. 469, 2018, doi: 10.1039/c7ee01987d.

[62] T. W. May, Y. M. Yeap, and A. Ukil, ‘Comparative evaluation of power loss in HVAC and HVDC transmission systems’, in *IEEE Region 10 Annual International Conference, Proceedings/TENCON*, Feb. 2017, pp. 637–641. doi: 10.1109/TENCON.2016.7848080.

[63] W. A. Amos, ‘Costs of Storing and Transporting Hydrogen’, Golden, 1998. Accessed: Aug. 04, 2022. [Online]. Available: http://www.doe.gov/bridge/home.html

[64] Palisade, ‘@RISK ’, 2022. https://www.palisade.com/risk/ (accessed Aug. 18, 2022).

APPENDICES

Appendix A – Seasonal wind speed distribution

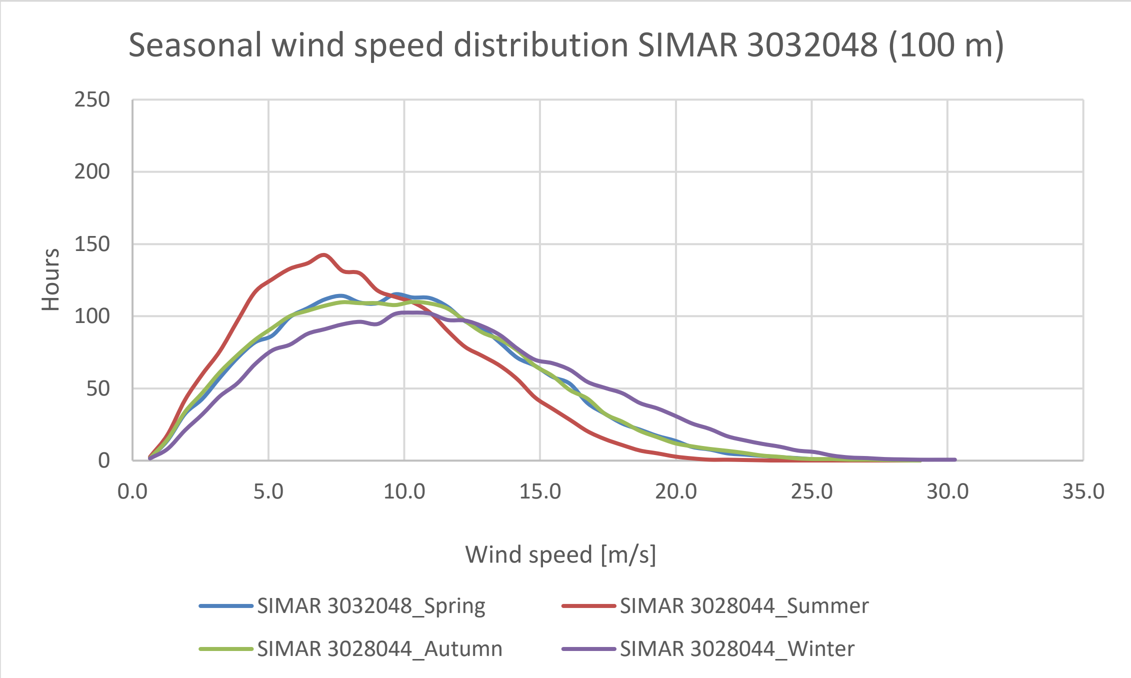

Figure A-1: Seasonal wind speed distribution SIMAR 2032048 (Galicia)

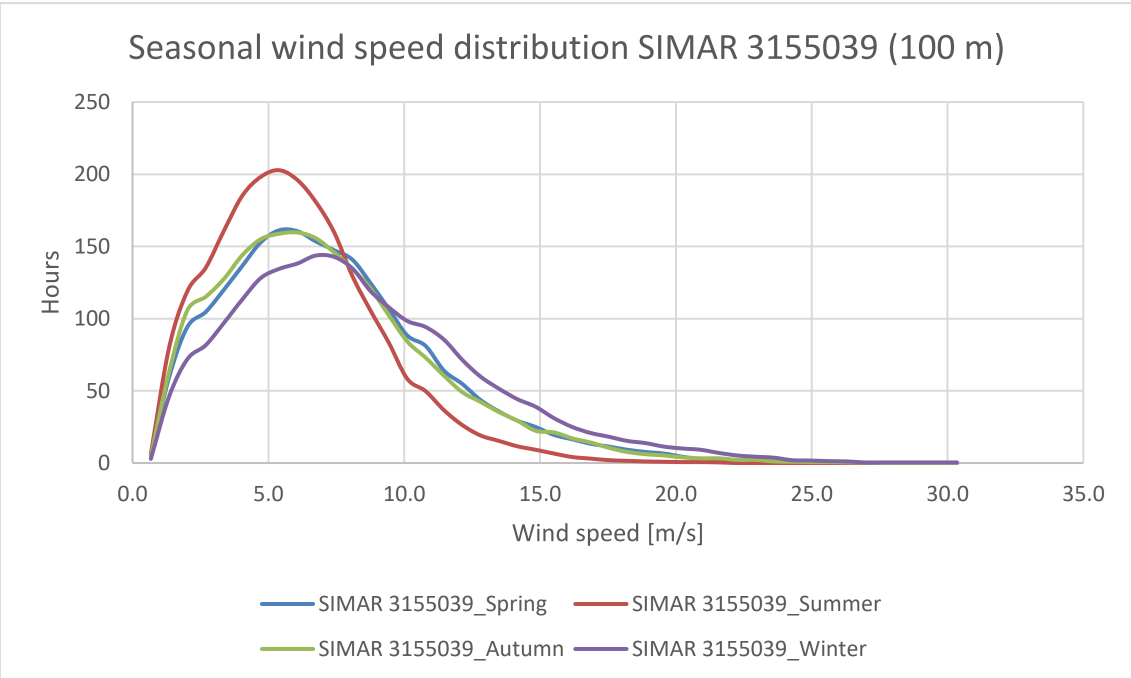

Figure A-2: Seasonal wind speed distribution SIMAR 3155039 (Bilbao)

Appendix B – Wind farm cost breakdown

B.1 Development and consenting

Table B-1: Development and consenting cost Galicia

GALICIA	Cost [M€]		
	V164-9.5	SG 8.0 - 167 DD	SWT - 4.0 - 130
G_-4	13.97	13.44	13.44
G_-3	15.96	15.12	14.28
G_-2	17.96	16.80	15.12
G_-1	19.95	18.48	15.96
G_0	21.95	20.16	16.80
G_1	23.94	21.84	17.64
G_2	25.94	23.52	18.48
G_3	27.93	25.20	19.32
G_4	29.93	26.88	20.16

Table B-2: Development and consenting cost Bilbao

BILBAO	Cost [M€]		
	V164-9.5	SG 8.0 - 167 DD	SWT - 4.0 - 130
B_-4	27.93	25.20	21.00
B_-3	29.93	26.88	21.84
B_-2	31.92	28.56	22.68
B_-1	33.92	30.24	23.52
B_0	35.91	31.92	24.36
B_1	37.91	33.60	25.20
B_2	39.90	35.28	26.04
B_3	41.90	36.96	26.88
B_4	43.89	38.64	27.72

B.2 Turbines and substructures

Table B-3: Turbines and substructures cost Galicia

GALICIA	Cost [M€]		
	V164-9.5	SG 8.0 - 167 DD	SWT - 4.0 - 130
G_-4	162.40	166.40	230.40
G_-3	185.60	187.20	244.80
G_-2	208.80	208.00	259.20
G_-1	232.00	228.80	273.60
G_0	255.20	249.60	288.00
G_1	278.40	270.40	302.40
G_2	301.60	291.20	316.80
G_3	324.80	312.00	331.20
G_4	348.00	332.80	345.60

Table B-4: Turbines and substructures cost Bilbao

BILBAO	Cost [M€]		
	V164-9.5	SG 8.0 - 167 DD	SWT - 4.0 - 130
B_-4	324.80	312.00	360.00
B_-3	348.00	332.80	374.40
B_-2	371.20	353.60	388.80
B_-1	394.40	374.40	403.20
B_0	417.60	395.20	417.60
B_1	440.80	416.00	432.00
B_2	464.00	436.80	446.40
B_3	487.20	457.60	460.80
B_4	510.40	478.40	475.20

B.3 Mooring

Table B-5: Mooring cost Galicia

GALICIA	Cost [M€]		
	V164-9.5	SG 8.0 - 167 DD	SWT - 4.0 - 130
G_-4	4.78	5.46	10.92
G_-3	5.46	6.14	11.60
G_-2	6.14	6.82	12.28
G_-1	6.82	7.51	12.96
G_0	7.51	8.19	13.65
G_1	8.19	8.87	14.33
G_2	8.87	9.55	15.01
G_3	9.55	10.23	15.69
G_4	10.23	10.92	16.38

Table B-6: Mooring cost Bilbao

BILBAO	Cost [M€]		
	V164-9.5	SG 8.0 - 167 DD	SWT - 4.0 - 130
B_-4	9.55	10.23	17.06
B_-3	10.23	10.92	17.74
B_-2	10.92	11.60	18.42
B_-1	11.60	12.28	19.10
B_0	12.28	12.96	19.79
B_1	12.96	13.65	20.47
B_2	13.65	14.33	21.15
B_3	14.33	15.01	21.83
B_4	15.01	15.69	22.52

B.4 Electrical infrastructure

B.4.1 Export cable and offshore platform

Table B-7: Export cable and offshore platform cost

Export cable + offshore platform cost [M€]	
Galicia	Bilbao
48.2	45.85

B.4.2 Transmission

Table B-8: Inter-array cable length Galicia

GALICIA	Inter-array cable length [km]		
	V164-9.5	SG 8.0 - 167 DD	SWT - 4.0 - 130
G_-4	11.32	15.41	25.65
G_-3	15.32	16.65	26.70
G_-2	16.54	17.88	27.75
G_-1	17.76	19.12	28.80
G_0	18.98	20.35	29.85
G_1	20.20	21.59	30.90
G_2	21.42	22.82	34.90
G_3	22.64	26.82	35.95
G_4	26.64	28.06	37.00

Table B-9: Inter-array cable length Bilbao

BILBAO	Inter-array cable length [km]		
	V164-9.5	SG 8.0 - 167 DD	SWT - 4.0 - 130
B_-4	22.64	26.82	38.05
B_-3	26.64	28.06	43.10
B_-2	27.86	29.29	44.15
B_-1	29.08	30.53	45.20
B_0	30.30	31.76	45.20
B_1	31.52	33.00	46.25
B_2	32.74	34.23	47.30
B_3	33.96	38.23	48.35
B_4	37.96	39.47	53.40

Table B-10: Transmission cost Galicia

GALICIA	Transmission costs [M€]		
	V164-9.5	SG 8.0 - 167 DD	SWT - 4.0 - 130
G_-4	1.69	2.30	3.82
G_-3	2.28	2.48	3.98
G_-2	2.46	2.66	4.13
G_-1	2.65	2.85	4.29
G_0	2.83	3.03	4.45
G_1	3.01	3.22	4.60
G_2	3.19	3.40	5.20
G_3	3.37	4.00	5.36
G_4	3.97	4.18	5.51

Table B-11: Transmission cost Bilbao

BILBAO	Transmission costs [M€]		
	V164-9.5	SG 8.0 - 167 DD	SWT - 4.0 - 130
B_-4	3.37	4.00	5.67
B_-3	3.97	4.18	6.42
B_-2	4.15	4.36	6.58
B_-1	4.33	4.55	6.73
B_0	4.51	4.73	6.73
B_1	4.70	4.92	6.89
B_2	4.88	5.10	7.05
B_3	5.06	5.70	7.20
B_4	5.66	5.88	7.96

B.4.3 Total

Table B-12: Total electricity transport cost Galicia

GALICIA	Total electricity transport costs [M€]		
	V164-9.5	SG 8.0 - 167 DD	SWT - 4.0 - 130
G_-4	49.88	50.49	52.02
G_-3	50.48	50.68	52.17
G_-2	50.66	50.86	52.33
G_-1	50.84	51.04	52.49
G_0	51.02	51.23	52.64
G_1	51.20	51.41	52.80
G_2	51.39	51.59	53.39
G_3	51.57	52.19	53.55
G_4	52.16	52.37	53.71

Table B-13: Total electricity transport cost Bilbao

BILBAO	Total electricity transport costs [M€]		
	V164-9.5	SG 8.0 - 167 DD	SWT - 4.0 - 130
B_-4	49.23	49.85	51.52
B_-3	49.82	50.03	52.27
B_-2	50.00	50.22	52.43
B_-1	50.18	50.40	52.59
B_0	50.37	50.58	52.59
B_1	50.55	50.77	52.74
B_2	50.73	50.95	52.90
B_3	50.91	51.55	53.06
B_4	51.51	51.73	53.81

B.5 Installation

Table B-14: Installation cost Galicia

GALICIA	Cost [M€]		
	V164-9.5	SG 8.0 - 167 DD	SWT - 4.0 - 130
G_-4	39.55	40.59	44.62
G_-3	40.57	41.08	45.08
G_-2	41.06	41.58	45.54
G_-1	41.55	42.07	46.00
G_0	42.05	42.57	46.46
G_1	42.54	43.06	46.92
G_2	43.03	43.56	47.94
G_3	43.52	44.58	48.40
G_4	44.54	45.07	48.86

Table B-15: Installation cost Bilbao

BILBAO	Cost [M€]		
	V164-9.5	SG 8.0 - 167 DD	SWT - 4.0 - 130
B_-4	39.55	40.61	45.34
B_-3	40.57	41.10	46.56
B_-2	41.06	41.60	47.02
B_-1	41.56	42.09	47.48
B_0	42.05	42.59	47.74
B_1	42.54	43.08	48.20
B_2	43.03	43.58	48.66
B_3	43.52	44.60	49.12
B_4	44.54	45.09	50.34

B.6 Decommissioning

Table B-16: Decommissioning cost Galicia

GALICIA	Cost [M€]		
	V164-9.5	SG 8.0 - 167 DD	SWT - 4.0 - 130
G_-4	14.24	14.55	18.49
G_-3	15.69	15.80	19.36
G_-2	17.09	17.06	20.24
G_-1	18.48	18.31	21.11
G_0	19.88	19.57	21.98
G_1	21.28	20.82	22.85
G_2	22.67	22.08	23.77
G_3	24.07	23.38	24.64
G_4	25.52	24.63	25.51

Table B-17: Decommissioning cost Bilbao

BILBAO	Cost [M€]		
	V164-9.5	SG 8.0 - 167 DD	SWT - 4.0 - 130
B_-4	23.74	23.05	26.05
B_-3	25.19	24.30	26.99
B_-2	26.58	25.56	27.86
B_-1	27.98	26.81	28.73
B_0	29.38	28.07	29.58
B_1	30.78	29.32	30.45
B_2	32.17	30.58	31.32
B_3	33.57	31.88	32.19
B_4	35.02	33.13	33.14

B.7 CAPEX

Table B-18: CAPEX Galicia

GALICIA	Cost [M€]		
	V164-9.5	SG 8.0 - 167 DD	SWT - 4.0 - 130
G_-4	284.81	290.92	369.89
G_-3	313.75	316.02	387.30
G_-2	341.70	341.11	404.70
G_-1	369.65	366.21	422.11
G_0	397.60	391.31	439.52
G_1	425.55	416.40	456.93
G_2	453.50	441.50	475.40
G_3	481.45	467.58	492.80
G_4	510.39	492.68	510.21

Table B-19: CAPEX Bilbao

BILBAO	Cost [M€]		
	V164-9.5	SG 8.0 - 167 DD	SWT - 4.0 - 130
B_-4	474.80	460.93	520.97
B_-3	503.74	486.03	539.81
B_-2	531.69	511.13	557.22
B_-1	559.64	536.22	574.62
B_0	587.58	561.32	591.66
B_1	615.53	586.42	609.07
B_2	643.48	611.51	626.48
B_3	671.43	637.59	643.89
B_4	700.37	662.69	662.72

B.8 OPEX

Table B-20: OPEX Galicia

GALICIA	Cost [M€/year]		
	V164-9.5	SG 8.0 - 167 DD	SWT - 4.0 - 130
G_-4	4.76	4.58	4.58
G_-3	5.44	5.15	4.87
G_-2	6.12	5.72	5.15
G_-1	6.80	6.30	5.44
G_0	7.48	6.87	5.72
G_1	8.16	7.44	6.01
G_2	8.84	8.01	6.30
G_3	9.52	8.59	6.58
G_4	10.20	9.16	6.87

Table B-21: OPEX Bilbao

BILBAO	Cost [M€/year]		
	V164-9.5	SG 8.0 - 167 DD	SWT - 4.0 - 130
B_-4	9.46	8.54	7.12
B_-3	10.14	9.11	7.40
B_-2	10.82	9.68	7.69
B_-1	11.49	10.25	7.97
B_0	12.17	10.82	8.25
B_1	12.84	11.39	8.54
B_2	13.52	11.95	8.82
B_3	14.20	12.52	9.11
B_4	14.87	13.09	9.39